nature reviews cardiology

https://doi.org/10.1038/s41569-025-01167-6

Review article

Check for updates

Mechano-energetic uncoupling in heart failure

Dunja Aksentijevic[1] ✉, Simon Sedej[2,3,4], Jeremy Fauconnier[5], Melanie Paillard[6], Mahmoud Abdellatif[2,3,7], Katrin Streckfuss-Bömeke[8,9], Renée Ventura-Clapier[10], Jolanda van der Velden[11], Rudolf A. de Boer[12], Edoardo Bertero[13], Jan Dudek[14], Vasco Sequeira[14] & Christoph Maack[14,15] ✉

Abstract

Heart failure (HF) is a major global and life-threatening disease. Despite advances in therapies, the prevalence of HF is increasing owing to an ageing population and the pervasive pandemic of obesity and metabolic disorders, which have transformed the pathophysiology of HF. Changes in cardiac energy metabolism and the related energy deficit crucially contribute to the severity and type of HF. Furthermore, perturbations in excitation–contraction coupling, mitochondrial function and oxidative stress are characteristic features of HF.

In this Review, we focus on the close interaction between cardiac mechanics and mitochondrial energetics, and decipher how this mechano-energetic coupling is disturbed in various acquired and hereditary forms of HF. In HF with reduced ejection fraction, defects in excitation–contraction coupling are key drivers of mechano-energetic uncoupling, whereas in HF with preserved ejection fraction, increased preload and afterload imposed by obesity, hypertension and age-dependent vascular stiffness increase mechanical workload, which is insufficiently matched by mitochondrial tricarboxylic acid cycle activity and ATP supply. In both scenarios, oxidative stress results from depletion of the antioxidative capacity and contributes to maladaptive cardiac remodelling and dysfunction. Several established and emerging treatments for HF target this mechano-energetic uncoupling, and a greater understanding of the underlying mechanisms will open new therapeutic opportunities to alleviate the burden of HF.

Sections

Introduction

Mechano-energetic coupling in the healthy heart

HFrEF

Hereditary cardiomyopathies

HFpEF

Sex-related differences in mechano-energetic uncoupling in HF

Disrupted NAD^+ metabolism as a treatable risk factor for HF?

Clinical translation of targeting mechano-energetic (un)coupling in HF

Conclusions

A full list of affiliations appears at the end of the paper. ✉e-mail: d.aksentijevic@qmul.ac.uk; maack_c@ukw.de

SHOUT
SHARE
IT

Key points

- Heart failure (HF) is characterized by defects in excitation–contraction (EC) coupling, energy deficits and oxidative stress; these defects are tightly intertwined by mechano-energetic coupling, and impairments in either EC coupling or mitochondrial function can induce a vicious cycle of events that results in maladaptive cardiac remodelling and dysfunction.
- The essence of mechano-energetic coupling is that oxidative phosphorylation for ATP production in mitochondria is regulated both by Ca^{2+}, stimulating tricarboxylic acid cycle activity and the respiratory chain from upstream ('push' condition), and by ADP, which accelerates respiration from downstream ('pull' condition).
- In HF with reduced ejection fraction, major defects lie in the alterations to EC coupling, in particular cytosolic Ca^{2+} and Na^{+} handling, impairing mitochondrial Ca^{2+} uptake and, consequently, the upstream 'push' conditions.
- In HF with preserved ejection fraction, pathological cardiac workload has an important role, inducing excessive 'pull' from downstream, which is aggravated by metabolic and mitochondrial dysfunction induced by metabolic diseases.
- Mechano-energetic uncoupling can also be an important driver of disease in hereditary cardiomyopathies, such as in hypertrophic cardiomyopathy, in which variants in genes encoding sarcomeric proteins increase the workload of cardiomyocytes (defective 'pull'), or in Barth syndrome, in which severe defects in mitochondrial Ca^{2+} uptake are observed (defective 'push').
- Therapeutic approaches are directed to normalizing the mechano-energetic imbalance, by adjusting workload, the defects in EC coupling or mitochondrial energetics.

Introduction

Heart failure (HF) is a global pandemic affecting at least 26 million people worldwide and is increasing in prevalence[1]. Comorbidities, such as obesity and diabetes mellitus, as well as demographic changes, exacerbate the cardiovascular disease burden, given that metabolic complications and ageing are major and independent risk factors for the development of HF[2–6]. Consequently, the lifetime risk of HF has increased to 24% (ref. 1). Prognosis remains poor: patients with HF have an average life expectancy of 2.5 years after their first hospitalization[7] and 50% die within 5 years after they are first diagnosed[8].

The healthy heart shows metabolic flexibility and is an 'omnivore', using primarily fatty acids, carbohydrates, amino acids, ketones and lactate as energy sources[9]. In patients with HF with reduced ejection fraction (HFrEF) or HF with preserved ejection fraction (HFpEF), lower phosphocreatine (PCr) to ATP ratios indicate an energy deficit, which is associated with reduced exercise capacity and, in the case of HFrEF, also with adverse outcome[10–13]. However, the concept of the failing heart as an 'engine out of fuel'[13] goes beyond a mere energy deficit and involves alterations in substrate utilization, intermediary metabolism, ATP phosphotransfer and mitochondrial redox regulation that collectively contribute to maladaptive cardiac remodelling and altered excitation–contraction (EC) coupling[14]. Equally, defects in EC coupling and pathological cardiac workload in HF impair the matching of energy supply and demand[15], in which the Krebs cycle (also known as the tricarboxylic acid cycle) has a key role[14,15]. Therefore, perturbations in cardiac metabolism must be analysed in an integrated fashion, considering the interaction between EC coupling and mitochondrial energetics.

Although targeting cardiac metabolism in patients with HF by switching substrate flux from fatty acids towards glucose oxidation proved to be unsuccessful in improving outcomes[16], important breakthroughs have been made in metabolic treatments for HF with sodium–glucose cotransporter 2 (SGLT2) inhibitors[17–20] and glucagon-like peptide 1 (GLP1) receptor agonists[21–24]. Unlike with neurohormonal blockers[25], the effectiveness of metabolic interventions is also seen in patients with a left ventricular (LV) ejection fraction (LVEF) ≥50%, providing clinical benefit to those with HFpEF[17,20]. Furthermore, novel compounds specifically targeting sarcomeres, such as cardiac myosin modulators[26–29], have further broadened our therapeutic armamentarium, allowing for more personalized and aetiology-driven approaches. Finally, the latest clinical and preclinical studies have broadened our insights into the haemodynamic and metabolic characteristics of patients with HFpEF, not only in relation to their comorbidity profile, but also compared with patients with HFrEF.

In this Review, we provide a comprehensive overview of the bidirectional interaction between EC coupling and mitochondrial energetics in cardiomyocytes, which we refer to as mechano-energetic coupling[30], a term that encompasses the effect of alterations in EC coupling and mechanical load on mitochondrial ion handling, redox state, reactive oxygen species (ROS) emission and substrate utilization, feeding back on cardiac function and morphology. In addition to established treatments for HF, we discuss the mechanisms and effects of novel therapeutic approaches, such as those targeting mitochondrial cardiolipin, ion handling or ROS, as well as aberrant nicotinamide adenine dinucleotide (NAD^{+}) homeostasis in various clinically relevant models of HF and, when applicable, in clinical studies involving patients with HF.

Mechano-energetic coupling in the healthy heart

EC coupling

Myocardial function is supported by continuous cardiac cycles subdivided into systole, comprising isovolumic contraction and ejection of blood, and diastole, comprising isovolumic relaxation and cardiac filling. Each of these phases is governed by the dynamic control of cytosolic Ca^{2+} cycling and the ATP:ADP ratio. During the initial phase of the cardiac action potential, voltage-gated Na^{+} channels open and depolarize the sarcolemma through Na^{+} influx. Subsequent Ca^{2+} entry into the cell through voltage-gated L-type Ca^{2+} channels triggers the release of even larger amounts of Ca^{2+} from the sarcoplasmic reticulum (SR) by activating ryanodine receptor 2 (RYR2) channels, a process termed Ca^{2+}-induced Ca^{2+} release[31] (Fig. 1). Released Ca^{2+} binds to cardiac troponin C, displacing the troponin–tropomyosin complex to unmask myosin-binding sites on the thin actin filament. In parallel, hydrolysis of ATP bound at the myosin head generates the driving energy for actin–myosin (crossbridge) interaction. As inorganic phosphate (P_i) is released, myosin remains weakly bound to actin (in the myosin–ADP–P_i state), maintaining myofilament inactivity. Myofilament activation occurs with the formation of strongly bound, force-producing crossbridges (in the myosin–ADP state), enabling a conformational 'power stroke' that slides actin filaments,

shortens sarcomeres and propels contraction[31]. Relaxation occurs when cytosolic Ca^{2+} decreases due to repolarization of the membrane potential (which limits entry of Ca^{2+} into the cell), inactivation of RYR2 (which stops the release of Ca^{2+} from the SR), removal of Ca^{2+} from the cytosol via the sarcolemmal Na^+–Ca^{2+} exchanger (NCX) to the extracellular space, and Ca^{2+} reuptake into the SR via the sarcoplasmic/endoplasmic reticulum Ca^{2+} ATPase 2a (SERCA2a) (Fig. 1). Myosin detachment from actin requires ADP dissociation and subsequent ATP binding. Additionally, mechanical crossbridge detachment is facilitated during cardiac filling.

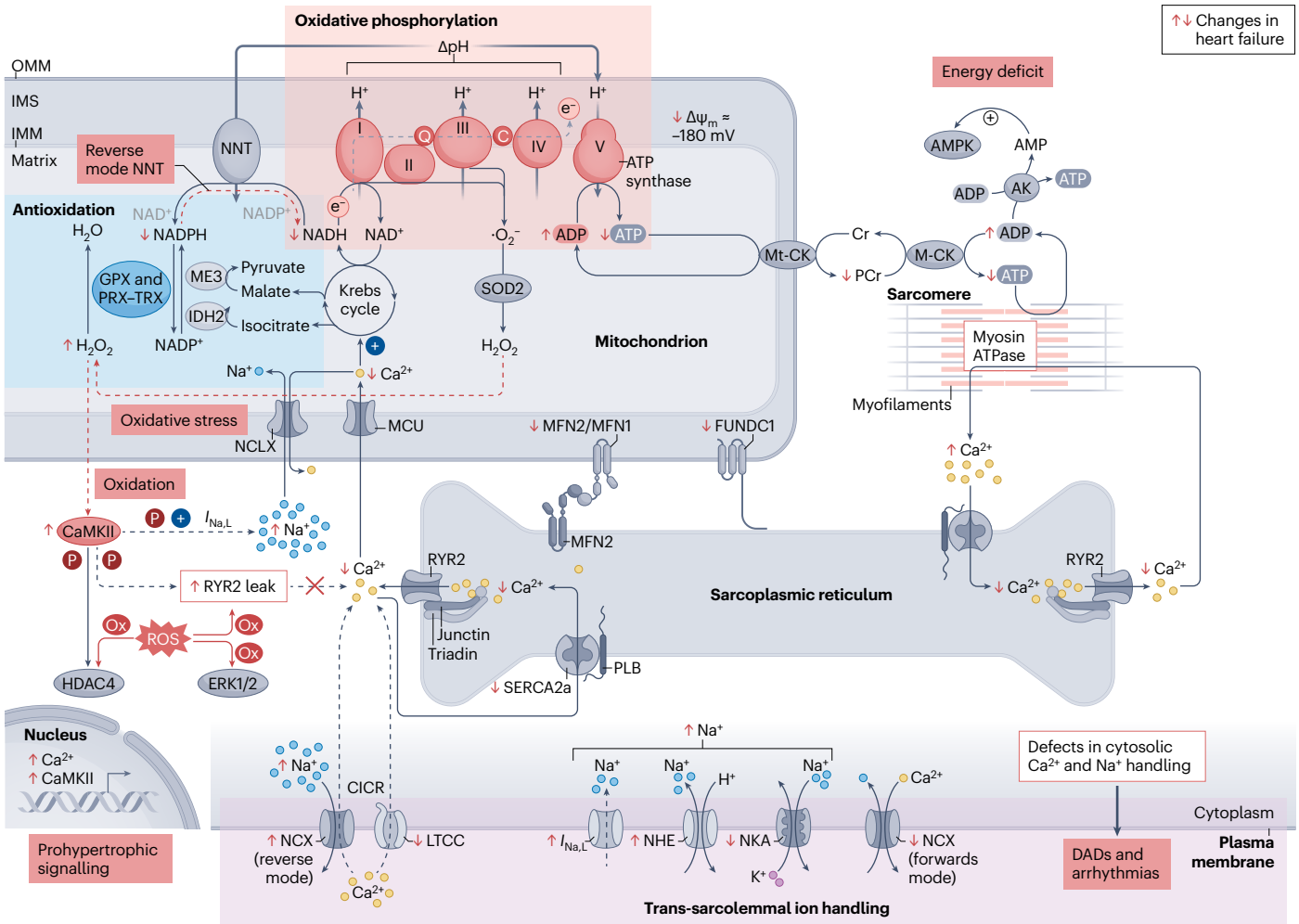

Fig. 1 | Mechano-energetic coupling in the healthy heart and uncoupling in HFrEF. Ca^{2+} entering the cell via L-type Ca^{2+} channels (LTCCs) stimulates Ca^{2+} release from the sarcoplasmic reticulum (SR) via ryanodine receptor 2 (RYR2) in a process known as Ca^{2+}-induced Ca^{2+} release (CICR). Mitochondria take up Ca^{2+} via the mitochondrial Ca^{2+} uniporter (MCU) and release it via the mitochondrial Na^+–Ca^{2+} exchanger (NCLX). Close contact points between the SR and mitochondria are controlled by SR-located mitofusin 2 (MFN2) tethered to MFN2 and/or MFN1 on the outer mitochondrial membrane (OMM), creating 'microdomains' of very high Ca^{2+} concentrations in the vicinity of mitochondria. Another SR–mitochondria tethering protein is FUN14 domain-containing protein 1 (FUNDC1). In the mitochondrial matrix, Ca^{2+} activates Krebs cycle dehydrogenases to regenerate NADH, which donates electrons to the respiratory chain. The electron flow produces a proton gradient (ΔpH) that drives ATP production at the F_1F_o ATP synthase (complex V). ATP converts creatine (Cr) to phosphocreatine (PCr) at the mitochondrial creatine kinase (Mt-CK), whereas in the cytosol, PCr regenerates ADP to ATP at myofilamental CK (M-CK). Superoxide ($\cdot O_2^-$) is generated at complex I and complex III of the respiratory chain and is transformed to H_2O_2 by mitochondrial superoxide dismutase (Mn) (SOD2). H_2O_2 is eliminated by glutathione peroxidase (GPX) and the peroxiredoxin (PRX)–thioredoxin (TRX) system. NADPH regenerates glutathione (GSH) from its oxidized form (GSSG) via glutathione reductase (GR). NADPH is regenerated by mitochondrial isocitrate dehydrogenase (NADP) (IDH2), mitochondrial NADP-dependent malic enzyme (ME3) and the mitochondrial NAD(P) transhydrogenase (NNT). The red arrows indicate the alterations that occur in heart failure, particularly heart failure with reduced ejection fraction (HFrEF). Increased production of H_2O_2 can oxidize Ca^{2+}–calmodulin-dependent protein kinase II (CaMKII), which in turn phosphorylates the Na^+ channel to increase the late Na^+ current ($I_{Na,L}$); other sources of increased Na^+ influx in HFrEF include increased activity of the Na^+–H^+ exchanger (NHE) or decreased activity of the Na^+–K^+ ATPase (NKA). Alterations in excitation–contraction coupling contribute to systolic and diastolic dysfunction, as well as arrhythmias, in HFrEF. Furthermore, increased levels of reactive oxygen species (ROS) can activate histone deacetylase 4 (HDAC4) or ERK1/ERK2, which can contribute to pro-hypertrophic signalling. AK, adenylate kinase; DAD, delayed afterdepolarization; IMM, inner mitochondrial membrane; IMS, intermembrane space; NCX, Na^+–Ca^{2+} exchanger; Ox, oxidation; P, phosphorylation; PLB, phospholamban; SERCA2a, sarcoplasmic/endoplasmic reticulum Ca^{2+} ATPase 2a.

Mitochondrial energetics and redox regulation

The processes of EC coupling require enormous amounts of ATP. In guinea pig hearts, 76% of this demand is used by the myosin ATPase, 15% by SERCA2a and 9% by Na^+–K^+ ATPase (NKA)[32]. Mitochondria are the dominant source of ATP in cardiomyocytes. In the mitochondrial matrix, the Krebs cycle is fuelled by glucose, fatty acids, ketones and amino acids[14]. The main products of the Krebs cycle are the reduced forms of NAD^+ (NADH) and flavine adenine dinucleotide ($FADH_2$), which donate electrons to complex I and complex II of the electron transport chain (ETC), initiating electron transfer via complex III to complex IV, where oxygen (O_2) is eventually reduced to water (H_2O) (Fig. 1). These sequential redox reactions promote proton translocation across the inner mitochondrial membrane, establishing a proton gradient, which together with the electrical gradient constitutes the proton-motive force that drives the rephosphorylation of ADP to ATP at the F_1F_o ATP synthase, a process called oxidative phosphorylation[15].

Even under physiological conditions, ~0.2% of O_2 is incompletely reduced at complexes I and III to generate superoxide anion radicals ($\cdot O_2^-$), which are transformed to hydrogen peroxide (H_2O_2) by mitochondrial superoxide dismutase (Mn) (SOD2)[33]. H_2O_2 is then eliminated by glutathione peroxidase (GPX), glutathione reductase (GR) and the peroxiredoxin–thioredoxin (PRX–TRX) system, which all require the reduced form of nicotinamide adenine dinucleotide phosphate (NADPH) to maintain their antioxidative capacity[34] (Fig. 1). NADPH, in turn, is regenerated by enzymes that derive their substrates from the Krebs cycle, such as mitochondrial isocitrate dehydrogenase (NADP) (IDH2), mitochondrial NADP-dependent malic enzyme and the mitochondrial NAD(P) transhydrogenase (NNT)[15] (Fig. 1). Given that the production of $\cdot O_2^-$ depends on NADH feeding electrons into the ETC[33], and the detoxification of ROS depends on the availability of reducing equivalents from NADPH[34], mitochondrial ROS emission is kept low in an intermediate redox state in the healthy working heart, according to the 'redox-optimized ROS balance' concept[35,36]. Therefore, any imbalance in the mitochondrial redox state owing to either excessive oxidation or reduction provokes an increase in the mitochondrial emission of ROS[35,36].

Mechano-energetic coupling

The heart adjusts its cardiac output under several physiological (such as exercise) and pathological (such as HF) conditions. This adjustment involves β-adrenergic stimulation and frequency-dependent potentiation of force (the Bowditch effect or force–frequency relationship), which typically occur together[37,38]. Furthermore, the Frank–Starling mechanism[30] and the slow force response[39] increase cardiac contractility in response to elevated cardiac preload, whereas the Anrep effect does so in response to an increase in cardiac afterload[40,41].

Under physiological conditions, cardiac output is mainly increased by β-adrenergic stimulation, which elevates the amplitude and frequency of cytosolic Ca^{2+} transients. The ensuing increase in ATP hydrolysis accelerates ADP flux to the mitochondria, stimulates ATP production at the F_1F_o ATP synthase and consumes electrons from NADH and $FADH_2$ to maintain the proton-motive force, inducing oxidation of NADH to NAD^+ and $FADH_2$ to FAD (the so-called pull condition)[42–45]. At the same time, the increase in the frequency and amplitude of cytosolic Ca^{2+} transients mediates mitochondrial Ca^{2+} uptake via the mitochondrial Ca^{2+} uniporter (MCU), and because of the much slower export of Ca^{2+} via the mitochondrial Na^+–Ca^{2+} exchanger (NCLX), Ca^{2+} accumulates in the mitochondrial matrix[42–45]. Elevation of mitochondrial Ca^{2+} levels from nanomolar to micromolar concentrations activates rate-limiting dehydrogenases of the Krebs cycle[46] as well as the F_1F_o ATP synthase[47], creating 'push' conditions in which electrons are pushed from NADH and $FADH_2$ into the respiratory chain to accelerate respiration[43]. At the same time, Ca^{2+}-induced acceleration of Krebs cycle dehydrogenases re-equilibrates the mitochondrial redox states of NADH–NAD^+ and $FADH_2$–FAD[42–45]. The fact that Ca^{2+} stimulates both the consumption and the regeneration of NADH, $FADH_2$ and ATP is referred to as parallel activation[48], thus highlighting a central role of mitochondrial Ca^{2+} handling in the homeostatic regulation of cardiac function and energetics[49]. Given that NADPH regeneration is also coupled to Krebs cycle products (Fig. 1), mitochondrial Ca^{2+} uptake also regenerates the antioxidative capacity during transitions of workload, preventing excessive mitochondrial emission of ROS[15,50].

Mitochondrial Ca^{2+} uptake is well established to shape cytosolic Ca^{2+} transients in non-cardiomyocytes[51], but the existence of this phenomenon in ventricular cardiomyocytes is arguably more controversial[44,45,52–54]. However, in atrial cardiomyocytes, which largely lack a transverse tubular system, subsarcolemmal mitochondria buffer the centripetal propagation of Ca^{2+} transients, thereby regulating atrial contractility[55]. Furthermore, perinuclear mitochondria in ventricular cardiomyocytes shape the perinuclear Ca^{2+}, probably preventing excessive nuclear Ca^{2+} uptake that governs transcription through activation of the nuclear Ca^{2+}–calmodulin-dependent protein kinase II (CaMKII)[56,57].

Mitochondrial Ca^{2+} handling

Mitochondrial Ca^{2+} uptake is a dynamic and electrophoretic process governed by three key parameters: the Ca^{2+} concentration gradients between the mitochondrial matrix and the cytosol, the mitochondrial membrane potential, and the presence of pores and channels to allow Ca^{2+} to cross both the outer and the inner mitochondrial membranes. Voltage-dependent anion channels (VDACs) provide the main route for Ca^{2+} to cross the outer mitochondrial membrane. Three different isoforms have been identified; VDAC1 and VDAC2 are mostly expressed in the heart and are less permeable to Ca^{2+} than VDAC3 (ref. 58). Therefore, the high expression of VDACs make the outer mitochondrial membrane relatively permeable to Ca^{2+}, giving the main control of Ca^{2+} uptake to the channels in the highly Ca^{2+}-impermeable inner mitochondrial membrane.

The MCU complex (MCUC) is a multiprotein complex located in the inner mitochondrial membrane and is formed by a tetramer of the pore-forming MCU subunits that confers the Ca^{2+} selectivity of the channel[59–62]. Permeability of the MCU is governed by incorporation of the mitochondrial essential MCU regulator (EMRE), a 10-kDa, single-pass membrane protein[63]. The ratio of EMRE to MCU varies from 1:4 to 4:4, depending on the tissue or cell type, providing a first level of regulation of channel conductance[64,65]. Furthermore, EMRE has a pivotal role in the electrostatic anchoring of regulatory subunits, namely the mitochondrial Ca^{2+} uptake proteins (MICUs), in the intermembrane space[63]. MICU1 comprises two Ca^{2+}-sensing EF hand domains and functions as a gatekeeper of the MCUC at low Ca^{2+} concentrations[66]. Additionally, MICU1 increases channel conductivity when cytosolic Ca^{2+} reaches micromolar concentrations in the vicinity of the complex[67]. MICU1 forms stable homodimers[68] or heterodimers with MICU2 (ref. 69) or MICU3 (ref. 70) via a disulfide bond. The two homologues (MICU2 and MICU3) have a similar Ca^{2+}-sensing structure, but require the presence of MICU1, the sole subunit that can bind to EMRE. MICU2 and MICU3 expression differs between tissues, with MICU3 being predominantly expressed in the brain[70]. This diversity extends the range of regulation of the MCUC, allowing fine tuning of

the MCUC sensitivity and cooperativity threshold in a tissue-specific manner[68,71–74]. Furthermore, under certain conditions, the MCUC can incorporate the dominant negative subunit MCUb, an MCU paralogue, which results in a reduction in channel conductance[75,76].

The composition of the MCUC, and in particular the ratios between MCU and its regulators, differs substantially between tissues, resulting in a wide range of MCUC current densities[54,77]. This heterogeneity provides a highly specific mitochondrial Ca^{2+} uptake pattern, optimized to match tissue-specific energy demand and cell-specific dynamics of cytosolic Ca^{2+} oscillations[78]. For example, the liver has a high MICU1:MCU ratio and, therefore, MCUC is strongly gated at low cytosolic Ca^{2+}, meaning that Ca^{2+} uptake is prevented at lower cytosolic Ca^{2+} concentrations. At higher cytosolic Ca^{2+} concentrations that supersede the threshold, mitochondrial Ca^{2+} uptake is more efficient (that is, high cooperativity). This strong gating and cooperativity ensure efficient mitochondrial fatty acid and glucose oxidation after food intake-induced cytosolic Ca^{2+} release[72,79]. By contrast, the heart and skeletal muscles have a low MICU1:MCU ratio, indicating a greater proportion of ungated MCU, which ensures basal Ca^{2+} uptake but relatively limited cooperativity at high cytosolic Ca^{2+} concentrations[72]. This muscle-specific MCUC composition might prevent Ca^{2+} overload caused by the large and constant Ca^{2+} oscillations encountered during EC coupling, thereby allowing the decoding of the Ca^{2+} spikes to promote efficient oxidative metabolism. Indeed, mice with a conditional cardiac knockout of *Mcu* have normal cardiac function at baseline but a blunted increase in cardiac contractility in response to β-adrenergic stimulation[49,80]. This finding demonstrates the crucial requirement of mitochondrial Ca^{2+} uptake to match ATP supply to demand during variations in cardiac workload.

The MCUC is a highly selective Ca^{2+} channel but has a low Ca^{2+} sensitivity and conductance[81,82]. To overcome this characteristic, the MCUC is located in specific microdomains in the vicinity of the SR of cardiomyocytes[83,84]. This specific SR–mitochondrial coupling comprises membrane apposition without fusion, forming mitochondria-associated reticular membranes and allowing close apposition of RYR2 to the MCUC. Mitochondria-associated reticular membranes are recognized as a signalling hub, with optimal transmission of Ca^{2+} between the SR and mitochondria occurring across a distance of 20–30 nm (ref. 85). Indeed, computational modelling predicts that the Ca^{2+} concentration at this distance from RYR2s is ≥30 μmol/l during SR Ca^{2+} release[86], sufficient to overcome the relatively low affinity of the MCUC for Ca^{2+} (refs. 81,82). Therefore, the efficiency of mitochondrial Ca^{2+} uptake is optimal when Ca^{2+} is released from the SR via this SR–mitochondria Ca^{2+} microdomain between RYR2 and the MCUC, which is particularly sustained during β-adrenergic stimulation when energetic requirements increase exponentially[44,53].

In cardiomyocytes, several proteins tether the SR to mitochondria. The Ca^{2+}-channelling complex formed by the reticular IP_3 receptor (IP_3R), the mitochondrial stress 70 protein (also known as GRP75) and VDAC stimulates mitochondrial ATP production[87]. Furthermore, the FUN14 domain-containing protein 1 (FUNDC1) interacts with IP_3R to increase Ca^{2+} transfer to mitochondria[88]. Finally, SR-located mitofusin 2 (MFN2) tethers with MFN2 or MFN1 on the outer mitochondrial membrane, supporting SR–mitochondria Ca^{2+} coupling[89].

Myocardial Na^+ regulation

In a healthy mammalian heart, the intracellular concentration of Na^+ ($[Na^+]_i$) is lower than its electrochemical equilibrium values. In large mammals, $[Na^+]_i$ is approximately 6–10 mmol/l, whereas in rats and mice, $[Na^+]_i$ ranges from 10 to 20 mmol/l (refs. 90–92). This higher $[Na^+]_i$ in smaller rodents is linked to physiological adaptations, such as higher heart rate and shorter action potential, making EC coupling less reliant on transmembrane Ca^{2+} flux and more on intracellular Ca^{2+} cycling[90,91]. These adaptations result in a flat force–frequency relationship and post-rest potentiation of SR Ca^{2+} release[93].

The low $[Na^+]_i$ in larger species is maintained by the NKA, which creates a transmembrane electrochemical gradient, acting as a 'battery' to drive ions and substrates across the cell membrane[90] (Fig. 1). During the cardiac contractile cycle, NKA uses ATP to transport Na^+ and K^+ across membranes, maintaining a strict stoichiometry. The activity of NKA must surpass the combined influx pathways to maintain this gradient. NKA is a transmembrane protein with α and β subunits located in the sarcolemma and transverse tubules. Phospholemman (PLM) is an important regulator of NKA, influencing cardiomyocyte contractility[90,91,94]. The activity of NKA is influenced by $[Na^+]_i$, with PLM exerting a tonic inhibition that is relieved by phosphorylation, primarily by protein kinase A and protein kinase C[94]. This regulation is crucial during changes in heart rate or adrenergic stimulation. Owing to its sarcolemmal localization and high demand for ATP, NKA is fuelled mainly by ATP derived from glycolysis[95,96].

CK phosphagen system

The amount of ATP needed to sustain EC coupling in the heart is enormous[15]. Paradoxically, however, the total amount of ATP stored in an adult human heart is only 0.6 g (ref. 97), barely sufficient for a few beats. This situation necessitates a rapid turnover of the entire ATP pool every ~10 s. To meet this demand, mitochondria comprise 40% of the cardiomyocyte volume, and the continuous provision of ATP is crucial to maintain normal cardiac output for approximately 3 billion heartbeats during a lifetime[98–100].

Central to the myocardial biochemical plasticity is the creatine kinase (CK) phosphagen system, which functions as an energetic shuttle and buffer in the cytosol[13,97,99]. Mitochondrial CK (Mt-CK) regenerates ATP in the intermembrane space, phosphorylating creatine (Cr) to PCr, which diffuses to the cytosol (Fig. 1). At the myofilaments, myofilament CK (M-CK) converts PCr and ADP into ATP, directly fuelling energy consumption at the site of demand. This system ensures rapid ATP regeneration, maintaining low cytosolic ADP levels and preserving the ATP:ADP ratio that is crucial for efficient mechano-energetic coupling[101].

In addition to CK, an auxiliary phosphotransfer network is governed by adenylate kinase (AK), which interconverts two ADP molecules to form ATP, P_i and AMP, which in turn can activate 5′-AMP-activated protein kinase (AMPK)[102]. AMP is dephosphorylated by 5′-nucleotidase to adenosine, which is lost from the cell via an equilibrative nucleoside transporter. Via multistep reactions, the pentose phosphate pathway provides ribose, which is necessary for de novo protein synthesis and replenishment of the adenine nucleotide pool (ATP, ADP and AMP)[99].

Taken together, high metabolic flexibility and mitochondrial density, coupled with dynamic control of oxidative phosphorylation by ADP and Ca^{2+} as well as an abundant CK–PCr buffer system guarantees constant ATP supply during the large variations in cardiac work under both physiological and pathological conditions.

HFrEF

Defects in EC coupling

In cardiomyocytes from animal models or patients with HFrEF, a key alteration in EC coupling is decreased SR Ca^{2+} load and release, mainly

caused by reduced activity and expression of SERCA2a, but also by leaky RYR2s[38,103,104] (Fig. 1). As a result, the amplitude of cytosolic Ca^{2+} transients is reduced, the rate of diastolic Ca^{2+} decay is slowed and diastolic Ca^{2+} concentrations are elevated[38,103]. In addition, $[Na^+]_i$ is elevated as a consequence of increased late Na^+ current ($I_{Na,L}$)[105,106] and Na^+–H^+ exchanger (NHE) activity[107,108], as well as changes in NKA expression and activity and PLM phosphorylation[90,109] (Fig. 1). Elevated $[Na^+]_i$ hinders cytosolic Ca^{2+} efflux via the forwards mode of the NCX. Conversely, high $[Na^+]_i$, together with decreased SR Ca^{2+} release, reverses the direction of the NCX during the early phase of the (prolonged) action potential to allow Ca^{2+} influx[110,111] (Fig. 1). Although this reversal partly compensates for decreased SR Ca^{2+} load to sustain inotropy of failing hearts[112], a pronounced contribution of NCX (versus L-type Ca^{2+} channel) to cytosolic Ca^{2+} influx slows the velocity of SR Ca^{2+} release and, consequently, the rate of increase of the cytosolic Ca^{2+} transient[113]. Together, these alterations slow the rates of contraction and relaxation of the failing myocardium and lower contractile force but increase diastolic tension, especially at higher heart rates, reversing the positive force–frequency relationship to a negative one[38,90,91,103]. Furthermore, the defects in EC coupling contribute to the higher vulnerability of failing hearts to the development of ventricular arrhythmias[103].

Defects in mitochondrial Ca^{2+} uptake

The defects in cytosolic Na^+ and Ca^{2+} handling in HFrEF negatively influence mitochondrial Ca^{2+} uptake and, consequently, mechano-energetic coupling. First, given that mitochondrial Ca^{2+} uptake crucially depends on coordinated Ca^{2+}-induced Ca^{2+} release from RYR2s into the SR–mitochondria Ca^{2+} microdomain, the decreased rate and amplitude of SR Ca^{2+} release diminishes mitochondrial Ca^{2+} uptake via the MCU[53] (Fig. 1). Second, reverse-mode NCX per se, but also NCX-triggered SR Ca^{2+} release, are less efficient for mitochondrial Ca^{2+} uptake owing to slower kinetics and a more remote location from mitochondria[53]. Third, elevated $[Na^+]_i$ accelerates mitochondrial Ca^{2+} export via NCLX, thereby lowering the steady-state $[Ca^{2+}]$ in the mitochondrial matrix[44] (Figs. 1 and 2).

In addition to disturbed EC coupling, alterations in mitochondrial localization and ion channel regulation also hamper mitochondrial Ca^{2+} uptake. First, Ca^{2+} uptake into isolated mitochondria via two distinct Ca^{2+} channels (then termed mCa1 and mCa2), reminiscent of the later-discovered MCU[60,62], is decreased in human failing versus non-failing myocardium[114]. As a potential explanation, the ratio of MICU1:MCU is increased in HFrEF in proportion to the degree of systolic dysfunction[115,116], favouring a higher MCU threshold and less mitochondrial Ca^{2+} uptake[72]. Furthermore, in a sheep model of HFrEF, the spatial organization of the SR with transverse tubules into dyads is disturbed, affecting the alignment of mitochondria with the SR[117]. Moreover, inter-mitochondrial tethering and, consequently, the network-like functional communication between mitochondria is disrupted in a guinea pig model of HFrEF[118], potentially related to downregulation of MFN2, rendering these mitochondria 'orphaned' from other mitochondria and the SR[119]. In the human failing myocardium, expression of the tethering protein FUNDC1 is decreased (Fig. 1), and mice with *Fundc1* deletion develop dilated cardiomyopathy (DCM)[88], supporting a causal role for disrupted SR–mitochondria Ca^{2+} coupling in the development of HFrEF. Furthermore, cardiomyocyte-specific deletion of *Mfn2* leads to DCM[89], but this finding might also be related to the additional role of MFN2 in governing mitophagy[120].

In addition to dysregulated tethering of the SR–mitochondria Ca^{2+} microdomain, mitochondrial transport and positioning in the cell is also affected. This positioning depends on the microtubular network, driven by kinesin motors[121]. In hypertrophied and failing human hearts, the microtubular network and its post-translational regulation are disturbed[122], which might also contribute to intracellular mislocalization of mitochondria. On the basis of their location, mitochondria are divided into subsarcolemmal, perinuclear and intermyofibrillar mitochondria[123]. In a mouse model of pressure overload-induced HFrEF, and also in human hearts, myofibrillar and perinuclear mitochondria are spatially disorganized in failing versus non-failing cardiomyocytes[57]. Together, these data demonstrate that alterations in EC coupling that occur in human HFrEF, involving changes in ion fluxes and the spatial organization of the organellar structure in cardiomyocytes, combine to impair mitochondrial Ca^{2+} uptake and accumulation.

Consequences of reduced mitochondrial Ca^{2+} uptake

Given that mitochondrial Ca^{2+} uptake has a central role in regulation of the Krebs cycle[15,48] and the respiratory chain[47], these defects have direct implications for mitochondrial redox state, energetics and ROS emission. In trabeculae isolated from the myocardium of patients with HFrEF, O_2 (and, therefore, ATP) consumption is similar to that in the non-failing myocardium, but consumed primarily by diastolic tension rather than systolic contraction[124]. Therefore, an energetic mismatch can be expected between ADP-induced acceleration of respiration and Ca^{2+}-induced regeneration of pyridine nucleotides by the Krebs cycle. Accordingly, diminished mitochondrial Ca^{2+} uptake oxidizes NADH and $FADH_2$ (refs. 44,50,125) (Fig. 1), contributing to the energy deficit in HFrEF[10,13]. In addition, NADPH oxidation in a guinea pig model of HFrEF depletes the antioxidative capacity, provoking excessive mitochondrial ROS emission[50] (Fig. 1). This oxidative stress can induce a broad array of downstream consequences, including further deterioration of EC coupling, arrhythmias, activation of redox-sensitive pro-hypertrophic signalling pathways (such as those involving CaMKII (ref. 126) and histone deacetylase 4 (ref. 127)) (Fig. 1) and induction of cell death[128]. In a mouse model of HFrEF, defective Ca^{2+} uptake into perinuclear mitochondria rendered these mitochondria more susceptible to membrane depolarization and ROS emission, and the loss of Ca^{2+} buffering by perinuclear mitochondria increased nucleoplasmic Ca^{2+} transients and accumulation[57], an upstream trigger for nuclear CaMKII activation and maladaptive remodelling[56] (Fig. 1).

Metabolic consequences of elevated $[Na^+]_i$

In addition to its effect on the mitochondrial redox state[44,50], high $[Na^+]_i$ also influences mitochondrial function and metabolism. Combined with increases in $I_{Na,L}$ and NHE activity, alterations in NKA function contribute to the elevation in $[Na^+]_i$[90,105–109]. NKA and metabolism have a bidirectional relationship[129]. Whereas declining ATP levels in HF can compromise ion transport, NKA inhibition and increased $[Na^+]_i$ can directly affect mitochondrial function[130] (Fig. 2). The reliance of NKA and SERCA2a on glycolytic metabolism might reflect attempts to maintain ion homeostasis in HFrEF, even if oxidative phosphorylation is compromised[90,129,130].

Studies using mouse heart perfusion and nuclear magnetic resonance spectroscopy indicate that elevated $[Na^+]_i$ alters metabolism even before the decline in energy reserves (PCr:ATP) and functional deterioration[129]. This finding was evident in models of either chronic or acute $[Na^+]_i$ elevation, including the PLM^{3SA} mouse model (in which PLM is rendered unable to be phosphorylated) with NKA inhibition, pressure overload-induced LV hypertrophy and pharmacological NKA inhibition

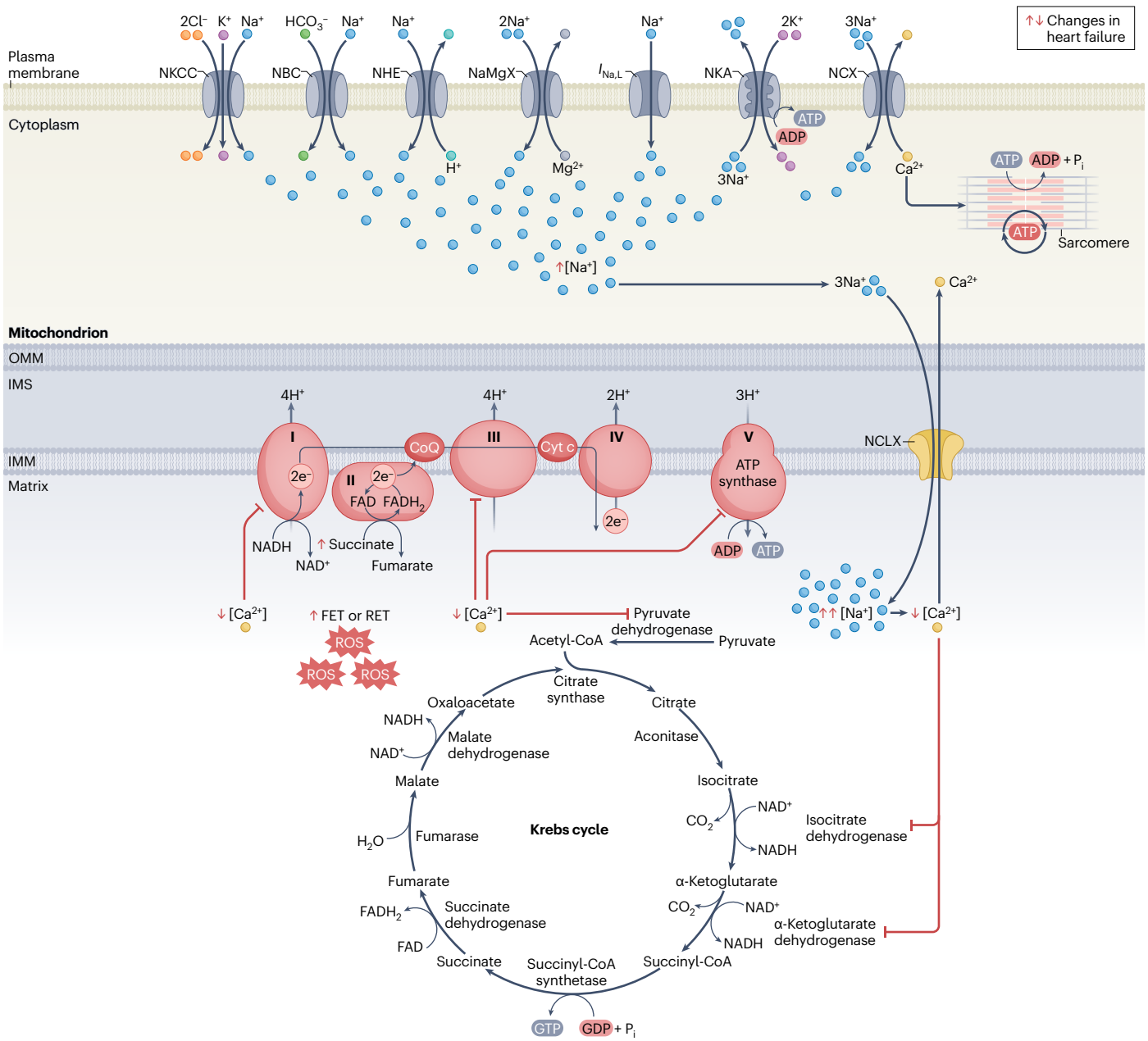

Fig. 2 | Effect of dysregulated cytosolic Na^+ handling on mitochondrial Ca^{2+} handling, the Krebs cycle and electron transport chain regulation. Na^+ entry into cardiomyocytes is regulated by several transporters. In the healthy heart, Na^+ channels ($I_{Na,L}$) and the Na^+–Ca^{2+} exchanger (NCX) are quantitatively the most important transporters. However, others might have a more prominent role in Na^+ overload in heart failure. The activity of Na^+–H^+ exchanger (NHE) and Na^+–HCO_3^- cotransporter (NBC) is increased during ischaemia–reperfusion due to the stimulation of proton extrusion by intracellular acidosis. Under mild acidosis (intracellular pH of 6.9), NHE and NBC can account for 75% of resting Na^+ influx. Other pathways for Na^+ entry are the Na^+–Mg^{2+} exchanger (NaMgX), which is involved in Mg^{2+} extrusion, and Na^+–K^+–$2Cl^-$ cotransporter (NKCC), which has a role in volume regulation. $[Na^+]_i$ is maintained at a low level by active pumping of Na^+ out of the cells by Na^+–K^+ ATPase (NKA). In pathological remodelling, an elevated cytoplasmic Na^+ concentration activates the mitochondrial Na^+–Ca^{2+} exchanger (NCLX), resulting in reduced Ca^{2+} levels in the mitochondrial matrix. This decrease impairs the function of Ca^{2+}-sensitive mitochondrial enzymes, including pyruvate dehydrogenase, mitochondrial isocitrate dehydrogenase (IDH2), α-ketoglutarate dehydrogenase, complex I, complex III and complex V (ATP synthase), subsequently impairing coenzyme Q (CoQ) recycling and causing an accumulation of $CoQH_2$. Excess $CoQH_2$ can promote the production of reactive oxygen species (ROS) via both forwards electron transport (FET) and reverse electron transport (RET) at complexes I and II. An elevated Na^+ concentration in the mitochondrial matrix also leads to succinate accumulation. Succinate accumulation can result from two potential mechanisms: limited availability of CoQ reduces complex II activity, impairing the oxidation of succinate to fumarate, or reverse electron transport at complex II drives the reduction of fumarate back to succinate. Cyt *c*, cytochrome *c*; IMM, inner mitochondrial membrane; IMS, intermembrane space; OMM, outer mitochondrial membrane; P_i, inorganic phosphate.

using ouabain[129]. All these models had a similar metabolic shift towards increased carbohydrate oxidation, which seemed adaptive because the PCr:ATP ratio and the NADH–NAD^+ redox state remained unaffected, whereas metabolic substrates such as lactate and amino acids were depleted, suggesting that this metabolic adaptation might not sustain a healthy PCr:ATP ratio in the long term[129]. In silico analyses revealed that, in response to elevated $[Na^+]_i$, the ATP supply is maintained through increased aerobic glucose metabolism and anaplerosis[129].

However, in these experiments, myosin ATPase (the main consumer of ATP) was partially inhibited with blebbistatin[129,130]. In the absence of such inhibition, with more ADP-induced acceleration of respiration, ouabain oxidizes NAD(P)H and increases mitochondrial ROS emission, because the ouabain-induced $[Na^+]_i$ elevation diminishes mitochondrial Ca^{2+} concentrations, establishing a mitochondrial redox mismatch[131] (Fig. 1). The increase in ROS triggers delayed afterdepolarizations in isolated cardiomyocytes and ventricular arrhythmias in isolated hearts and in vivo[131]. Together, these studies show that both acute and chronic elevations in $[Na^+]_i$ switch mitochondrial substrate utilization and hamper mechano-energetic coupling, resulting in oxidative stress that compromises EC coupling and induces arrhythmias (Figs. 1 and 2).

High $[Na^+]_i$ also leads to a reduced Ca^{2+} concentration in the mitochondrial matrix, resulting in suppressed activity of complex III, decreased recycling of coenzyme Q (CoQ) and a build-up of $CoQH_2$. Excess electrons in the $CoQH_2$ pool can lead to ROS generation via either forwards or reverse electron transport at complex I and complex II (ref. 130) (Fig. 2). Furthermore, elevated $[Na^+]_i$ leads to the intracellular accumulation of succinate by two potential mechanisms: limited availability of CoQ reduces complex II activity, impairing the oxidation of succinate to fumarate, and reverse electron transport at complex II drives the reduction of fumarate back to succinate[130] (Fig. 2). Elevated levels of succinate inhibit prolyl hydroxylases, thereby stabilizing hypoxia-inducible factor 1α by preventing its degradation[130].

Finally, $[Na^+]_i$ also regulates oxidative phosphorylation and mitochondrial ROS production more directly by altering the fluidity of the inner mitochondrial membrane[132]. During acute hypoxia, Na^+ enters the mitochondrial matrix via the NCLX, interacting with phospholipids to reduce membrane fluidity and limit ubiquinone mobility between complex II and complex III of the respiratory chain, increasing $\cdot O_2^-$ production at complex III (ref. 132). Whether this mechanism is also involved in the more moderate but chronic elevations in $[Na^+]_i$ in HF is uncertain.

Targeting mitochondrial Na^+, Ca^{2+} and redox regulation in HFrEF

Given that elevated $[Na^+]_i$ has such a central role in controlling mitochondrial redox state and metabolism, targeting the NCLX, which exports Ca^{2+} from mitochondria in exchange for Na^+, should correct many of the defects described above. Indeed, the NCLX inhibitor CGP-37157 increases mitochondrial Ca^{2+} accumulation in non-failing[44] and failing[125] cardiomyocytes; restores NAD(P)H oxidation[125] and prevents mitochondrial ROS emission[50] in failing cardiomyocytes; and prevents ouabain-induced NAD(P)H oxidation, ROS emission, delayed afterdepolarizations and ventricular arrhythmias in vivo[131]. NCLX inhibition also prevented the ouabain-induced switch in cardiac metabolism from fatty acids to glucose oxidation[129]; the decrease in the activities of respiratory chain complexes I, II and III; the accumulation of Krebs cycle products and also the ensuing decrease in Gibb's free energy of ATP hydrolysis[130]. In isolated mitochondria, CGP-37157 prevented the negative effect of high Na^+ concentrations on the fluidity of the inner mitochondrial membrane[132]. Finally, in vivo treatment with CGP-37157 prevented the development of systolic dysfunction and lethal ventricular arrhythmias in a guinea pig model of HFrEF[133].

Alternatively, increasing mitochondrial Ca^{2+} uptake by adenoviral overexpression of the MCU (by 60%) in the same guinea pig model of HFrEF improved systolic function and prevented ventricular arrhythmias and cardiac decompensation[134]. Activation of the MCU by the natural flavonoid kaempferol increased mitochondrial Ca^{2+} uptake and diminished the occurrence of atrial fibrillation[135]. Finally, given that elevated $[Na^+]_i$ and decreased mitochondrial Ca^{2+} uptake increase mitochondrial ROS emission[50], the mitochondria-targeted antioxidant Mito-TEMPO also prevented systolic dysfunction and ventricular arrhythmias in the guinea pig model of HFrEF[136]. Accordingly, in cardiomyocytes from a rabbit model of HFrEF, inhibiting mitochondrial ROS, $I_{Na,L}$ or CaMKII all prevented cellular arrhythmias[137].

Taken together, these data (mostly obtained in animal models of HFrEF with relatively low $[Na^+]_i$ under physiological conditions) indicate that $[Na^+]_i$ elevation has a causal role in the development of HFrEF and arrhythmias via impaired mitochondrial Ca^{2+} uptake and accumulation, provoking mitochondrial oxidation, ROS emission and metabolic remodelling. These findings indicate that targeting $[Na^+]_i$ or the NCLX might be an attractive strategy to ameliorate mechano-energetic uncoupling, maladaptive cardiac remodelling, systolic dysfunction and ventricular arrhythmias in HFrEF.

Species-dependent and injury-dependent differences in mitochondrial Ca^{2+} handling

Mechano-energetic uncoupling in HFrEF is distinct from the scenario of mitochondrial Ca^{2+} overload during cardiac ischaemia–reperfusion injury[138]. In the latter scenario, ATP depletion during ischaemia induces cytosolic and subsequently mitochondrial Ca^{2+} overload[138,139]. Together with a burst of ROS production on reperfusion, this Ca^{2+} overload opens the mitochondrial permeability transition pore (MPTP), initiating necrotic cell death[138,140]. However, in several mouse models of HFrEF, mitochondrial Ca^{2+} overload was also reported[141], such as in response to overexpression of L-type Ca^{2+} channels[142], genetic defects in respiratory chain function[143] or permanent myocardial infarction[144]. In the first model, the upstream cause of mitochondrial Ca^{2+} overload is a rather artificial cytosolic Ca^{2+} overload[142], whereas in post-ischaemic HF, mitochondrial Ca^{2+} overload can be traced to increased SR Ca^{2+} leak via oxidized RYR2 (ref. 144), which in another study could be rescued by accelerating mitochondrial Ca^{2+} export by overexpressing the NCLX[115].

What could be the reasons for these species-dependent differences? Mice have tenfold higher heart rates at rest (~600 bpm) than humans (~60 bpm), whereas during exercise, the increase in cardiac output and, accordingly, the required increase in ATP production are approximately tenfold lower in mice (0.5-fold increase[145,146]) than in humans (fivefold increase[147,148]). These differences have at least two implications. First, given that mitochondrial Ca^{2+} uptake is the key mechanism to adapt ATP supply to demand[15,48], less mitochondrial Ca^{2+} uptake might be required in mice than in humans. Accordingly, deletion of *Mcu* in mouse hearts produced no phenotype at rest and only a mildly blunted contractile reserve during β-adrenergic stimulation[49,149]. Second, to avoid mitochondrial Ca^{2+} overload at such high (resting) heart rates, mitochondrial Ca^{2+} extrusion must be optimized in mice. This optimization is partly achieved by a high $[Na^+]_i$ (approximately 10–20 mmol/l (refs. 90–92)), which maximizes NCLX activity[150]. In addition, transient openings of the MPTP also contribute

to mitochondrial Ca^{2+} extrusion, given that deficiency of cyclophilin D (a key component of the MPTP) also induces a lethal cardiomyopathy phenotype with excessive mitochondrial Ca^{2+} overload in response to pressure overload[151] (similar to deletion of the NCLX, encoded by *SLC8B1* (ref. 115)). These differences between mice and larger animals or humans need to be considered when interpreting the results of studies in mice with genetic modifications of mitochondrial Ca^{2+}-handling proteins[152].

Mechano-energetic uncoupling in response to increased cardiac afterload

Whereas defects in mitochondrial Ca^{2+} uptake and accumulation hamper 'push' conditions by compromising Ca^{2+}-induced Krebs cycle activation and regeneration of reducing equivalents, an excessive increase in 'pull' conditions can induce similar mechano-energetic uncoupling despite unchanged mitochondrial Ca^{2+} uptake (Fig. 3). In patients with HF, neuroendocrine activation and age-dependent vascular stiffening increase cardiac afterload.

In isolated hearts and in vivo, elevated afterload increases O_2 (and ATP) consumption[153] and, consequently, ADP-induced oxidation of NADH[154]. This change, together with ADP-induced and F_1F_o ATP synthase-mediated dissipation of the mitochondrial membrane potential, reverses the direction of the NNT, meaning that NADPH regenerates NADH towards ATP production, but at the cost of the NADPH-coupled antioxidative capacity[154] (Fig. 1). The ensuing increase in mitochondrial H_2O_2 emission induces necrotic and apoptotic cell death, maladaptive cardiac remodelling and contractile dysfunction[154]. C57BL/6J mice, but not C57BL/6N mice, have a loss-of-function variant in *Nnt*, protecting these mice from afterload-induced left-sided and right-sided HF[154–156].

Under physiological conditions, an acute increase in cardiac afterload triggers an increase in cardiac contractility via the Anrep effect in an effort to maintain stroke volume despite the increase in afterload[41,157]. Although separating the Frank–Starling mechanism, the so-called slow force response and the Anrep effect from one another is challenging when acutely increasing cardiac afterload in vivo[41], a pure

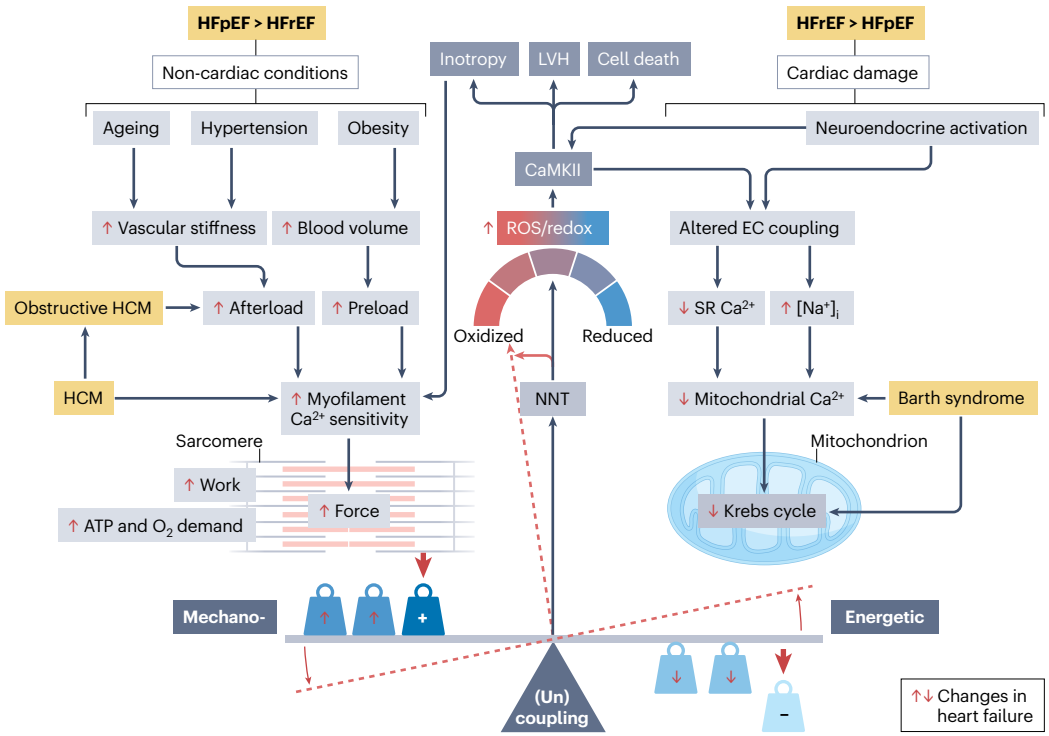

Fig. 3 | Mechano-energetic uncoupling in heart failure. In heart failure with preserved ejection fraction (HFpEF), ageing and hypertension increase vascular stiffness and thereby afterload, whereas obesity increases blood volume and thereby preload, both increasing myofilament Ca^{2+} sensitivity. This elevated Ca^{2+} sensitivity increases cardiomyocyte force generation, but also ATP demand and oxygen (O_2) consumption. This increased 'pull' condition is not adequately matched by Krebs cycle activation ('push' condition), resulting in a mismatch between ATP supply and demand. In addition, a redox mismatch increases mitochondrial emission of reactive oxygen species (ROS), which can activate Ca^{2+}–calmodulin-dependent protein kinase II (CaMKII) to sustain inotropy, but also promote the development of left ventricular hypertrophy (LVH) and, if excessive, can mediate cell death. In heart failure with reduced ejection fraction (HFrEF), hypocontractility is often caused by initial cardiac damage (such as cell death during myocardial infarction, myocarditis or toxic effects of chemotherapy or alcohol). Neuroendocrine activation in the long term dysregulates excitation–contraction (EC) coupling, in particular leading to decreased sarcoplasmic reticulum (SR) Ca^{2+} load and Ca^{2+} release, as well as an elevated cytosolic Na^+ concentration ($[Na^+]_i$). These alterations converge to hamper mitochondrial Ca^{2+} uptake and accumulation, which in turn impair Krebs cycle activation during workload transitions, causing oxidation of NADH and NADPH, which reduces the antioxidative capacity and allows elevated emission of ROS. In hypertrophic cardiomyopathy (HCM), variants in genes encoding sarcomeric proteins commonly increase myofilament Ca^{2+} sensitivity, which is further aggravated by an increase in afterload through the Anrep effect, and together increase mechanical workload without sufficient adaptation by Ca^{2+}-induced activation of the Krebs cycle[40,203]. In Barth syndrome cardiomyopathy, diminished mitochondrial Ca^{2+} uptake as a primary mitochondrial consequence of tafazzin deficiency impairs Ca^{2+}-induced activation of the Krebs cycle, and this mechano-energetic uncoupling is further aggravated by increased myofilament Ca^{2+} sensitivity, probably as a post-translational event[241]. NNT, mitochondrial NAD(P) transhydrogenase.

afterload-induced potentiation of force in a working heart system (in the absence of increased preload) involves increased myofilament Ca^{2+} sensitivity and oxidation and activation of CaMKII (ref. 157), which sustains contractility[158] but can induce maladaptive cardiac remodelling, failure and arrhythmias in the long term[159] (Fig. 3). Although increases in afterload in vivo can involve additional mechanisms, such as promotion of nitric oxide (NO) production by NO synthase 1 (NOS1) and ROS production by NADPH oxidase 2 (NOX2)[41] via activation of surface mechanosensors, activation of CaMKII (ref. 126) by mitochondrial ROS generated by reverse-mode NNT[154] might be an important mechanism underlying the 'pure' Anrep effect[157] (Figs. 1 and 3). These mechanisms might be sustained in the long term in patients (for example, those with obstructive hypertrophic cardiomyopathy)[40] and the ageing population[160].

CK phosphotransfer system in HFrEF

The defects in mechano-energetic coupling have consequences for the CK phosphotransfer system. In the 1930s, post-mortem studies identified low Cr levels in failing hearts[161]. Since then, numerous studies in humans[10–13,162,163] and across other species have revealed reductions in the levels of intracellular Cr, PCr and the PCr:ATP ratio, as well as of CK activity, regardless of HF aetiology. For instance, in a pig model of pressure overload, the total Cr level decreased by 26% and CK activity by 48% (ref. 164). In a dog pacing model of HFrEF, Cr levels and CK activity were reduced by 39% and 25%, respectively[165]. In this dog model, the loss of Cr and ATP was progressive, correlating with pacing duration. The decline in intracellular Cr level in HF might be compensatory, preventing ADP levels from rising and thereby maintaining the ATP:ADP ratio, which helps to preserve ΔG_{ATP} (the change in Gibbs free energy (G) of the ATP hydrolysis reaction) and slow the loss of adenine nucleotides[166].

A reduction in PCr levels or experimental inhibition of CK activity in rat hearts and isolated cardiomyocytes leads to hypercontractility and diastolic dysfunction, potentially linked to an ADP-induced increase in myofilament Ca^{2+} sensitivity[167], and is directly associated with the development of HF[167,168]. However, the reduction in CK activity is partially offset by alternative phosphotransfer pathways, such as that controlled by AK[169] (Fig. 1). In the dog pacing model of HFrEF, the contribution of AK to ATP turnover increased by 21%, and in mouse models of myocardial infarction and pressure overload, the contributions of AK and glycolytic pathways also increased relative to that of CK[170].

The observed decline in Cr levels in pathological remodelling is attributable to reduced Cr uptake, with expression of the creatine transporter 1 downregulated in both human and rat HF[171,172]. In the dog pacing model of HFrEF, M-CK and Mt-CK expression and activity were downregulated[166,173,174].

Increased M-CK acetylation, observed in human HF and mouse models of HF, inversely correlated with protein activity, suggesting acetylation–deacetylation pathways as potential therapeutic targets[175]. In human HFrEF, the PCr:ATP levels are decreased and predict an adverse outcome[10], and ATP flux through the CK system is reduced[163] and correlates with the decay in cardiac mechanical work and efficiency[162], indicating a direct link between energy deficit and contractile dysfunction in HFrEF. Indeed, unloading with a LV assist device increased CK activity and protein expression[176]. However, mice lacking Cr (and, therefore, CK activity) have normal cardiac function at rest and even during exercise[177], suggesting that mechanisms other than PCr deficiency per se contribute to contractile dysfunction in HF and/or redundant systems can compensate for this loss. Further understanding of the mechanisms governing the regulation of CK and creatine transporter 1 could clarify the link between HF and altered energetics and identify potential therapeutic targets.

Hereditary cardiomyopathies

A greater understanding of the genetic causes of hereditary cardiomyopathies and the translation of experimental technologies for use in diagnostics, as well as the use of genetically modified mouse models and patient-specific human induced pluripotent stem cell systems, are providing deeper insights into the pathophysiology of these diseases[178]. Given that many cardiomyopathy-causing variants affect genes encoding proteins involved in EC coupling, metabolism or mitochondrial function with various phenotypes[178–180], a wealth of novel insights into mechano-energetic defects in these cardiomyopathies has been gained, which might also educate us about the mechanisms underlying acquired forms of HF.

In this section, we highlight two hereditary cardiomyopathies that affect either the sarcomere (hypertrophic cardiomyopathy (HCM)) or mitochondria (Barth syndrome) and for which we have robust evidence that mechano-energetic uncoupling is a key pathophysiological mechanism.

HCM

HCM is the most common inherited cardiac disease[181], characterized by abnormal septal hypertrophy, hypercontractility, diastolic dysfunction[179,182,183] and ventricular arrhythmias that can cause sudden cardiac death[183,184]. In the majority of patients, HCM is caused by variants in genes encoding sarcomeric proteins, such as β-myosin heavy chain (βMHC; also known as myosin 7)[185], cardiac myosin-binding protein C (cMyBPC)[186,187], cardiac troponin T (cTnT)[187] and others[179]. These variants commonly increase myofilament Ca^{2+} affinity, which explains the presentation of hyperdynamic contraction and impaired relaxation[188] (Figs. 3 and 4). Given that this increased affinity also raises the energetic cost of EC coupling[189,190], PCr:ATP ratios decrease (and ADP levels increase) in the cardiomyocytes of patients with HCM[191,192], even before symptoms[193] or LV hypertrophy[194] develop, with more severe metabolic compromise in patients with familial versus non-familial HCM[195], and physical exercise aggravating energetic deficiency[196]. Similarly, in a mouse model with an HCM-typical variant in *Myh6* (encoding αMHC)[197], the PCr:ATP ratio was decreased, confirming the causal relationship between variants in genes encoding sarcomeric proteins and energy deficiency (Fig. 4). In patients with more advanced HCM, comprehensive omics and functional studies revealed mitochondrial dysfunction and oxidative stress correlating with the severity of the disease[198–202]. However, the mechanisms of how sarcomeric variants induce mitochondrial dysfunction and oxidative stress are largely unresolved[183].

In mice with HCM-typical mutations in *Mybpc3* or *Tnnt2*, the increased Ca^{2+} affinity of the myofilaments drains ATP reserves, and ADP-induced NADH oxidation reverses the NNT reaction to regenerate NADH from NADPH, supporting ATP production at the cost of NADPH oxidation[203], in a similar manner to that which occurs in response to an increase in cardiac afterload[154] (Figs. 1, 3 and 4). The ensuing increase in mitochondrial H_2O_2 emission triggers spontaneous Ca^{2+} release events from the SR and cytosolic Ca^{2+} waves, providing a trigger for arrhythmias[203]. The increased ATP demand causes focal energy deprivation that increases susceptibility to arrhythmias as a result of slowed conduction via dephosphorylation of connexin 43 (ref. 204), which could be prevented by elamipretide (also known as Bandavia, MTP-131 or SS-31; a tetrapeptide that binds to mitochondrial cardiolipin in mitochondria[205,206]). Ventricular arrhythmias were abolished ex vivo by

the NCLX inhibitor CGP-37157 and in vivo by the mitochondria-targeted antioxidant mitoquinone mesylate (MitoQ)[203]. In myectomy samples from patients with HCM, elamipretide or NAD^+ supplementation boosted mitochondrial respiration[202]. Together, these data indicate that mechano-energetic uncoupling caused by a mismatch between too much ATP consumption for any given level of mitochondrial Ca^{2+} uptake triggers and sustains ventricular arrhythmias[203] (Figs. 3 and 4), a frequent cause of death in patients with HCM[183,184].

Mitochondrial ROS generation resulting from mechano-energetic uncoupling is also likely to contribute to maladaptive cardiac remodelling in HCM (Fig. 4). ROS can activate CaMKII (ref. 126), and CaMKII is activated by autophosphorylation in the myocardium of patients with sarcomere variant-positive HCM[207–209] and in animal models of HCM[209–211]. CaMKII activation affects cytosolic Ca^{2+} and Na^+ handling in cardiomyocytes from mice and humans with HCM, such as increased $I_{Na,L}$[207] as a canonical mediator of CaMKII-induced arrhythmias[212], and can also induce cardiac hypertrophy via specific phosphorylation of histone deacetylase 4 (ref. 213), which can also be oxidized directly[127] (Figs. 1 and 4).

Redox-dependent activation of the Ras–Raf–MEK1/MEK2–ERK1/ERK2 signalling pathway also induces cardiomyocyte hypertrophy and sarcomere disorganization[214] (Fig. 4). Genetic variants in this signalling pathway cause RASopathies, a common cause of HCM in children[215]. In mouse models of RASopathies, pharmacological inhibition of MEK or ERK prevents the development of HCM[216], indicating that ERK1/ERK2 activation is a key downstream step that integrates pro-hypertrophic

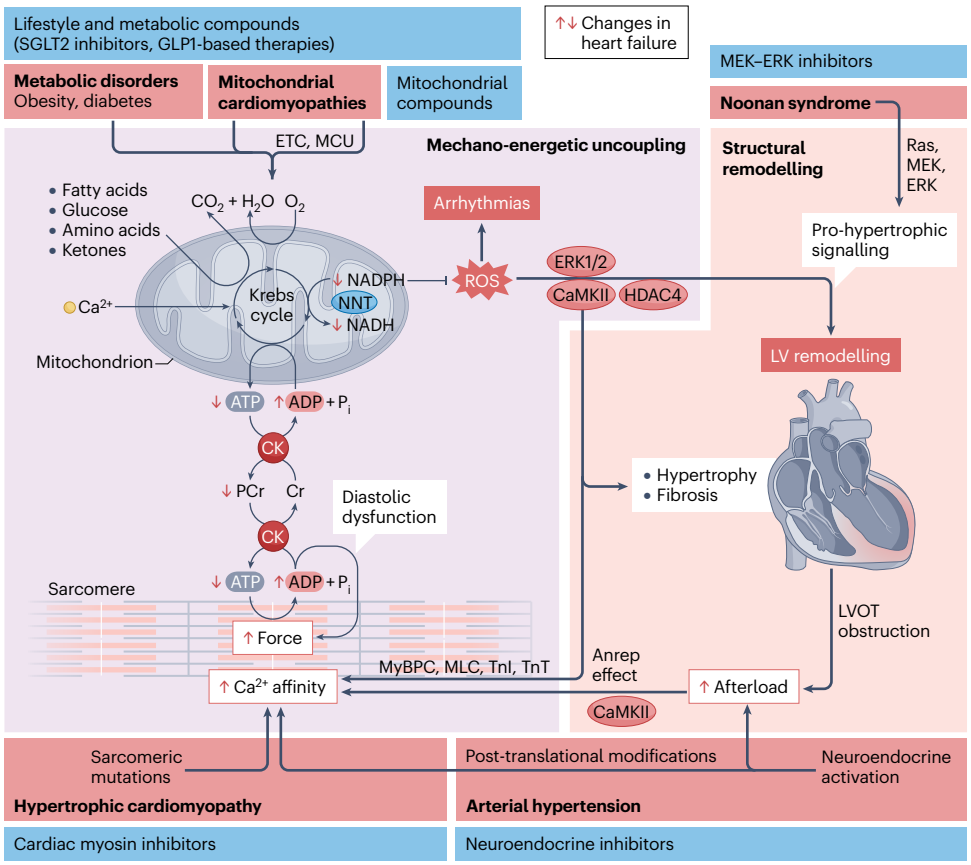

Fig. 4 | Different aetiologies of heart failure and cardiomyopathy converge on a shared pathophysiological trait of mechano-energetic uncoupling that drives cardiac remodelling and dysfunction. A vicious cycle of events that can start at any point drives the progression of heart failure. Increased workload imposed on sarcomeres, either by elevated afterload or by genetic variants or post-translational modifications of sarcomeric proteins, drain ATP from mitochondria, where a mismatch occurs due to insufficient Ca^{2+}-induced matching of Krebs cycle activity (see also Fig. 3). The ensuing oxidation of NADPH causes emission of reactive oxygen species (ROS) that can activate pro-hypertrophic signalling cascades, such as Ca^{2+}–calmodulin-dependent protein kinase II (CaMKII), histone deacetylase 4 (HDAC4) and extracellular signal-regulated kinase 1 (ERK1) or ERK2. These pathways account for cardiomyocyte hypertrophy, and probably also cardiac fibrosis and potentially myocardial inflammation. In hypertrophic cardiomyopathy (HCM), progressive left ventricular (LV) hypertrophy eventually leads to progressive (and often dynamic) obstruction of the LV outflow tract (LVOT), increasing afterload. The increase in afterload further increases myofilament Ca^{2+} affinity via the Anrep effect and thereby imposes an additional mechanical burden on sarcomeres and an energetic burden on mitochondria, exacerbating the mechano-energetic uncoupling. Potential causes of elevations in afterload other than obstructive HCM include aortic valve stenosis, stiffening of large arteries (during ageing) and neuroendocrine activation that leads to vasoconstriction. Various aetiologies of HFpEF and also HFrEF can converge on this shared pathophysiological trait, and aetiology-related treatments (as shown in the figure), can ameliorate disease progression. CK, creatine kinase; Cr, creatine; ETC, electron transport chain; GLP1, glucagon-like peptide 1; MCU, mitochondrial Ca^{2+} uniporter; MLC, myosin light chain; MyBPC, myosin-binding protein C; NNT, mitochondrial NAD(P) transhydrogenase; PCr, phosphocreatine; P_i, inorganic phosphate; SGLT2, sodium–glucose cotransporter 2; TnI, cardiac troponin I; TnT, cardiac troponin T.

signals from RAS pathways and ROS sources. Indeed, in animal models of HCM, ERK1/ERK2 activation[217], LV hypertrophy[218] and LV fibrosis[218,219] were reversed by the antioxidant *N*-acetylcysteine, a precursor of glutathione. ERK1/ERK2 determines the mode of hypertrophy (concentric versus eccentric[220]), corresponding to the degree of myofilamental Ca^{2+} sensitization in mouse models of HCM versus DCM[221]. Together, these studies suggest that mitochondrial ROS, as a consequence of mechano-energetic uncoupling, in addition to causing arrhythmias, might also be a cause of pathological cardiac hypertrophy in HCM (Fig. 4). Indeed, targeting mitochondrial (but not cytosolic) ROS reduced hypertrophy, fibrosis and diastolic dysfunction in a mouse model of LV hypertrophy[222,223].

When HCM and LV hypertrophy progress, an obstruction of the LV outflow tract (LVOT) develops in two-thirds of patients with HCM through bulging of the hypertrophied septum and systolic anterior motion of the mitral valve, which is then termed obstructive HCM[224]. This LVOT obstruction elevates afterload and LV end-systolic pressure, intensifying hyperdynamic contraction, myocardial O_2 demand, diastolic dysfunction and secondary mitral regurgitation, thereby increasing the risk of HF and sudden cardiac death[225]. This additional afterload on the sarcomeres aggravates mechano-energetic uncoupling, oxidative stress, myofilament Ca^{2+} sensitivity, CaMKII activation and maladaptive cardiac remodelling[154,157], creating a vicious cycle in which excessive mechanical work provokes ROS-induced cardiac remodelling and dysfunction (Fig. 4). Clinically, the afterload-induced force potentiation through the Anrep effect manifests chronically in patients with obstructive HCM, indicated by a leftwards shift and steepening of the end-systolic pressure–volume relationship and a prolonged systolic ejection time[40].

Although treatment with β-adrenoceptor blockers or Ca^{2+} channel blockers ameliorates symptoms, septal reduction therapy by alcohol septal ablation[226] and/or surgical myectomy is more efficient in reducing the LVOT gradient and, consequently, improving outcomes in patients with obstructive HCM[180]. Reduction of the LVOT gradient by alcohol septal ablation reverses Anrep-related hypercontractility[40]. Cardiac myosin inhibitors target the disease-causing mechanism even further upstream by directly targeting sarcomeric hypercontractility[29,227] (Fig. 4). The first-in-class drug, mavacamten, improved diastolic function by stabilizing the super-relaxed state of myosin, which also reduced inotropy[29,227]. The drug reversed maladaptive cardiac remodelling, myofibrillar disarray and fibrosis in a mouse model of HCM[227]. In patients with obstructive HCM, mavacamten and aficamten each reduced LVOT obstruction and improved symptoms, exercise capacity and LV geometry despite a modest, but desired, reduction in LVEF[27,28,228–231]. Taken together, these data indicate that both sarcomeric variants and LVOT obstruction in obstructive HCM converge to increase myofilament Ca^{2+} affinity and, consequently, cardiac workload, which through mechano-energetic uncoupling provokes the production of mitochondrial ROS that contribute to maladaptive cardiac remodelling and arrhythmias. However, reduction of sarcomeric workload through alcohol septal ablation or treatment with myosin inhibitors reverses these processes (Fig. 4).

Barth syndrome

Barth syndrome is a mitochondrial cardiomyopathy caused by variants in the *TAFAZZIN* gene encoding tafazzin (TAZ), a transacylase governing the remodelling of cardiolipin, a crucial phospholipid in the inner mitochondrial membrane that stabilizes protein complexes, such as components of the ETC[232]. Clinically, Barth syndrome is characterized by early onset cardiomyopathy, skeletal myopathy, neutropenia and growth delay[233]. Cardiomyopathy often presents as DCM, with high mortality in the first days of life, but then develops towards a phenotype with normal-sized ventricles, a LVEF of ~50% with blunted inotropic reserve and an increased risk of ventricular arrhythmias[234–236]. Studies on human induced pluripotent stem cell-derived cardiomyocytes from patients with Barth syndrome revealed that defective cardiolipin remodelling disrupts ETC supercomplexes, impairing respiration and increasing mitochondrial ROS production, resulting in systolic dysfunction[237,238]. Mice with complete *Tafazzin* knockout also have oxidative stress, increased CaMKII oxidation and hyperphosphorylation of RYR2, provoking spontaneous SR Ca^{2+} release, delayed afterdepolarizations, ventricular arrhythmias and the development of DCM[239,240].

In mice with *Tafazzin* knockdown and low residual TAZ expression, the cardiac phenotype is less severe, with normal-sized left ventricles and only mildly reduced LVEF (~50%), but diastolic dysfunction and blunted β-adrenergic reserve[241], resembling the more stable clinical phenotype in patients who survive beyond the first months of life[234–236]. In the absence of cardiac fibrosis, diastolic dysfunction is driven by increased myofilament Ca^{2+} affinity, which is partly compensated for by SERCA2a activation through reduced phospholamban expression, accelerating the rates of cytosolic Ca^{2+} decay at rest, but blunting the inotropic response to β-adrenergic stimulation[241] (Fig. 5). In mitochondria, a primary defect is severe downregulation of the MCU[241–243], which abolishes Ca^{2+}-induced Krebs cycle activation during workload transitions[241]. The ensuing oxidation of mitochondrial NAD(P)H and $FADH_2$ triggers cellular arrhythmias and slows ventricular conduction in vivo, which are both blunted by inhibiting the NCLX to boost mitochondrial Ca^{2+} accumulation[241]. However, despite NADPH oxidation, no increase in mitochondrial ROS was observed[241,244], probably related to a compensatory metabolic rewiring and boosted antioxidative capacity (Fig. 5) triggered by the integrated stress response, converging on the cAMP-dependent transcription factor ATF4 (ref. 245). Together, these data indicate that Barth syndrome cardiomyopathy is characterized by mechano-energetic uncoupling due to mitochondrial defects of the ETC and MCUC, which combine to alter mitochondrial redox signalling, resulting in arrhythmias and impaired ventricular function (Fig. 5).

Approaches to treat Barth syndrome that have been tested preclinically include small molecules, gene therapy and enzyme replacement therapy[246]. In the *Tafazzin*-knockdown model, adeno-associated virus (AAV) gene therapy strategies improved mitochondrial morphology and function as well as cardiac and skeletal muscle function[247]. In the more severely affected *Tafazzin*-knockout models, neonatal AAV gene therapy with human *TAFAZZIN* prevented neonatal death and cardiac dysfunction and fibrosis when cardiomyocyte transduction was ≥70% (ref. 239). The mitochondria-targeted agent elamipretide binds to cardiolipin and protects it from oxidative damage, which preserves mitochondrial function and reduces oxidative stress, without being an antioxidant in its own right[206]. Elamipretide treatment improved mitochondrial morphology, dynamics and function in hearts from *Tafazzin*-knockdown mice, but whether this treatment also improved cardiac function was uncertain[248,249]. In clinical trials involving patients with Barth syndrome, cardiac remodelling was reversed and LV stroke volume was improved after 3 years of open-label elamipretide treatment compared with baseline; the 6-min walking distance was improved after 36 weeks and 168 weeks (but not after 12 weeks) of elamipretide treatment[250,251]. Elamipretide has

been submitted to the FDA for approval for the treatment of patients with Barth syndrome.

HFpEF

The prevalence of HFpEF has been continuously increasing for at least the past four decades[252], making it the dominant form of HF, especially in older individuals[253–255]. Although mortality is similar between HFrEF and HFpEF[256], the contribution of non-cardiovascular causes of death is higher in patients with HFpEF[253], which is related to population ageing and a higher burden of comorbidities than in patients with HFrEF[257]. Compared with HFrEF, patients with HFpEF tend to be older, are more often female, are less likely to have an ischaemic cause of HF and have lower plasma levels of N-terminal pro-B-type natriuretic peptide (NT-proBNP)[258]. Although comorbidities such as obesity, diabetes, renal dysfunction and hypertension tend to be more common in patients with HFpEF, the differences in prevalence to patients with HFrEF are small[257].

Haemodynamics in HFpEF

Patients with HFrEF or HFpEF share a diminished capacity to increase cardiac output during exertion[259–263]. This reduced capacity is primarily related to β-adrenergic desensitization and downregulation in patients with HFrEF[263], but in patients with HFpEF might be related to a partial exploitation of the contractile reserve under resting conditions[259–262]. Both biased[264] and unbiased[265] approaches have revealed that patients with HFpEF can be categorized into two haemodynamic phenotypes. One is reminiscent of HFrEF, with an enlarged left ventricle and mild hypocontractility: reduced LV active contractility (measured in mmHg/ml) and a LVEF of 50–60%, but reduced systemic and pulmonary vascular resistance[264,265]. Some of or all these patients might

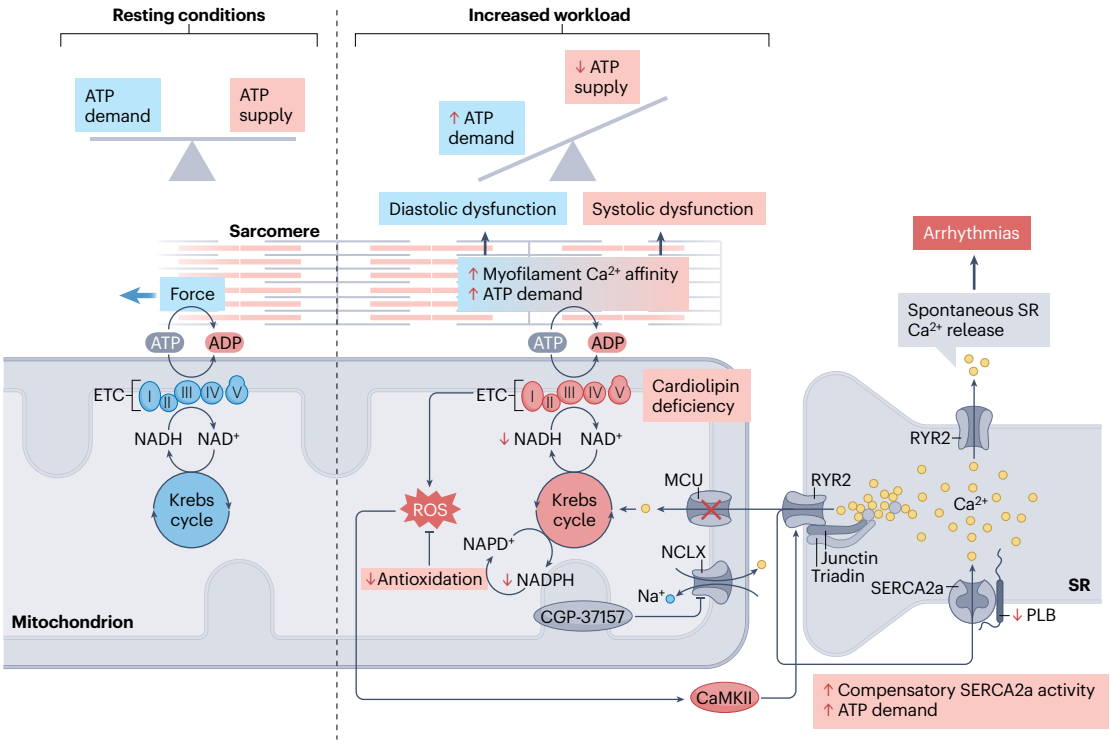

Fig. 5 | A unifying concept of mechano-energetic uncoupling in Barth syndrome. *Tafazzin*-knockdown mice have a low expression of tafazzin and a phenotype of heart failure with preserved ejection fraction[241], reminiscent of patients with Barth syndrome after the first months to years of life[234]. Evidence from this mouse model and data from human myocardium samples or induced pluripotent stem cell-derived cardiomyocytes suggest that the lack of mitochondrial Ca^{2+} uptake due to defects in the mitochondrial Ca^{2+} uniporter (MCU) affects the adaptive stimulation of mitochondrial metabolism and impairs energy and redox homeostasis during β-adrenergic stimulation[241,243]. Elevated myofilament Ca^{2+} affinity and slowed crossbridge cycling cause diastolic dysfunction[241]. A compensatory increase in the activity of sarcoplasmic/endoplasmic reticulum Ca^{2+} ATPase 2a (SERCA2a), induced by hyperphosphorylation of phospholamban (PLB), elevates energy demand even further and increases the energetic burden on mitochondrial metabolism[241]. Preactivated PLB–SERCA2a activity also limits the contractile reserve during β-adrenergic stimulation, resembling the clinical phenotype of a blunted increase in left ventricular ejection fraction during exertion in patients with Barth syndrome[241]. The *Tafazzin*-knockdown model does not have an elevation in mitochondrial reactive oxygen species (ROS) production, probably related to a compensatory rewiring of metabolism towards fuelling glutathione-dependent antioxidative systems[245]. *Tafazzin*-knockout mice have no expression of tafazzin and a phenotype of heart failure with reduced ejection fraction (that is, dilated cardiomyopathy)[239,240]. These mice have increased ROS production and ROS-dependent activation of Ca^{2+}–calmodulin-dependent protein kinase II (CaMKII), which in turn phosphorylates ryanodine receptor 2 (RYR2), giving rise to spontaneous Ca^{2+}-release events from the sarcoplasmic reticulum (SR), which can trigger cellular and whole-heart arrhythmias[240]. Oxidation of NADPH during β-adrenergic stimulation, as observed in the *Tafazzin*-knockdown model[241], might contribute to CaMKII oxidation, given that cellular arrhythmias were observed in these mice that could be prevented by boosting mitochondrial Ca^{2+} uptake through inhibition of mitochondrial Ca^{2+} export via the mitochondrial Na^{+}–Ca^{2+} exchanger (NCLX) with CGP-37157 (ref. 241). CL, cardiolipin; ETC, electron transport chain.

previously have had HFrEF, and their LVEF increased in response to therapy (so-called HF with improved ejection fraction). By contrast, patients with 'true' HFpEF have small hearts but high systemic and pulmonary vascular resistance, imposing a high afterload on both ventricles and demanding steeper slopes of end-systolic elastance (the end-systolic pressure–volume relationship), resulting in a typical LVEF of ≥60% (refs. 264,265).

Bioenergetic considerations in HFpEF

In terms of the underlying cellular processes, an increased afterload (as is observed in patients with HFpEF[264,265]) might increase contractility through mechano-energetic uncoupling, mitochondrial ROS and CaMKII activation[154,157], but also via increased myofilament Ca^{2+} sensitization[157], resembling, to some extent, the cellular alterations that occur in patients with (obstructive) HCM (Fig. 3). In LV[266] and right ventricular[267] biopsy samples from patients with HFpEF, myofilament Ca^{2+} affinity and sarcomere stiffness were elevated compared with healthy controls and could be reversed to levels observed in individuals without HFpEF by the cardiac myosin inhibitor mavacamten, pointing to increased actin–myosin interactions in HFpEF. This observation is consistent with the finding that mavacamten improved diastolic function and reduced plasma NT-proBNP and troponin levels in patients with HFpEF enrolled in the EMBARK-HFpEF trial[268]. Furthermore, in atrial cardiomyocytes from patients with HFpEF, CaMKII expression, phosphorylation and activity were increased and contributed to cellular Na^+ influx via $I_{Na,L}$[269]. In one mouse model of HFpEF, CaMKII inhibition reversed the prolonged action potential duration[270] and, in another, the PCr:ATP ratio was decreased, mitochondrial respiration was impaired and ROS emission was increased[271]. The elevated afterload and associated increase in contractility demand larger amounts of ATP, which is illustrated by a twofold increase in myocardial O_2 consumption and coronary blood flow in patients with HFpEF compared with healthy control individuals at rest (Fig. 3), thereby limiting the contractile, metabolic and coronary reserve to draw on during exercise[272].

Effect of obesity on the HFpEF phenotype

In the general population, obesity increases the risk of developing HFpEF but not HFrEF[273] and, in patients with HFpEF, obesity increases the risk of worsening HF but not mortality[274]. A major haemodynamic aspect of obesity is that adipocytes release adipokines[275], in particular leptin[276], which stimulate the production of aldosterone in the adrenal glands[275–277]. Na^+ and water retention expand plasma volume by ~40% and, consequently, cardiac output, driven largely by an increase in stroke volume, related to recruitment of the preload reserve mediated by the Frank–Starling mechanism[277–279] (Fig. 3). At the same time, however, the increased plasma volume elevates biventricular filling pressures at rest and during exercise[279,280]. In addition to (direct) activation of aldosterone synthesis, leptin also mediates activation of the renin–angiotensin–aldosterone and sympathetic nervous systems, which further contributes to the increase in cardiac output at rest[277], and these pathways collectively contribute to the substantial increase in cardiac mass in patients with obesity either with[279] or without[278] HFpEF.

On a cellular level, mitochondrial lipid accumulation and sarcomeric destruction can be observed in right ventricular biopsy samples from patients with HFpEF and severe obesity (BMI of ~40 kg/m^2), resulting in lower maximal force generation, despite elevated myofilament Ca^{2+} sensitivity[267,281]. Furthermore, an increase in preload, similar to an increase in afterload[154], oxidizes mitochondrial NAD(P)H owing to the elevated demand for ATP that is unmatched by mitochondrial Ca^{2+} uptake[42–44] (Fig. 3). These data indicate that the combination of elevated afterload, obesity and the associated elevation in preload increases myofilament Ca^{2+} affinity and mechano-energetic uncoupling, further aggravating the clinical and cardiac (cardiomyocyte) phenotype (Figs. 3 and 4). This phenomenon is also reflected in preclinical models, in which typically neither hypertension nor obesity alone but only the combination of the two mediates the HFpEF phenotype[282], such as in the most commonly used mouse model of HFpEF induced by the combination of a high-fat diet and application of the NOS inhibitor L-NAME (N_ω-nitro-L-arginine methyl ester)[283]. Interestingly, in this HFpEF model, the missense variant in *Nnt* in C57BL/6J mice ameliorates (or delays) the development of HFpEF, in contrast to C57BL/6N mice without the *Nnt* variant[284], corroborating the concept that mechano-energetic uncoupling with NNT-mediated NADPH oxidation and mitochondrial ROS emission might be a central element for the development of HFpEF (Figs. 3 and 4).

Taken together, studies on hereditary cardiomyopathies and HFpEF suggest that mechano-energetic uncoupling, characterized by hypercontractile sarcomeres but inadequate ATP supply from mitochondria, might be a shared downstream pathomechanistic trait that elicits a feedforward vicious cycle of hyperdynamic contraction and mitochondrial redox alterations that cause impairments in EC coupling, arrhythmias and maladaptive cardiac remodelling with progressive cardiac dysfunction (Figs. 3–5).

Defects in mitochondrial Ca^{2+} uptake in HFpEF

In addition to the increased haemodynamic burden, which aggravates the 'pull' conditions that drain the Krebs cycle products NADH, NADPH and $FADH_2$ (ref. 43), impairments in the 'push' conditions of Ca^{2+}-induced Krebs cycle activation can also occur in cardiometabolic HFpEF (Fig. 3). Reduced mitochondrial Ca^{2+} uptake with an increased MICU1:MCU ratio was reported in atrial cardiomyocytes in a mouse model of atrial fibrillation induced by a high-fat and high-sugar diet[135]. In another mouse model of high-fat and high-sugar diet-induced early metabolic HFpEF, reversible SR–mitochondria Ca^{2+} uncoupling triggered lower mitochondrial Ca^{2+} levels and bioenergetics in LV cardiomyocytes[285]. In a mouse model of type 1 diabetes, MCU expression and mitochondrial Ca^{2+} uptake were reduced, whereas AAV-mediated upregulation of MCU expression restored mitochondrial Ca^{2+} uptake, pyruvate dehydrogenase activity, mitochondrial respiration, and systolic and diastolic cardiac function[286]. Interestingly, decreased SR–mitochondria Ca^{2+} coupling was confirmed in LV biopsy samples from patients with type 2 diabetes, aortic valve stenosis and diastolic dysfunction but preserved LVEF, together with genetic remodelling of the MCUC towards a decreased MICU1:MCU ratio, potentially acting as a compensatory response[287]. Finally, in a rat model of pressure overload, modest (but not high) adenoviral overexpression of the MCU ameliorated mitochondrial ROS levels and prevented arrhythmias[286]. Taken together, reduced mitochondrial Ca^{2+} uptake might contribute to the development of HFpEF (Fig. 3). However, increased mitochondrial Ca^{2+} levels and uptake were reported in an obese ZFS1 rat model of metabolic HFpEF, with no change in MCU protein expression (MICU1 protein levels were not assessed)[288]. Further investigation is needed to validate whether alterations in mitochondrial Ca^{2+} handling per se contribute to mechano-energetic uncoupling and the progression of HFpEF.

Sex-related differences in mechano-energetic uncoupling in HF

Given that female patients are generally under-represented in clinical trials, recommendations for the diagnosis and treatment of patients

with HF are largely based on data obtained in male patients. However, important sex-related differences in epidemiology, pathophysiology, clinical course and treatment response of HF exist[255,289]. Men are more likely to develop ischaemic or non-ischaemic HFrEF, whereas women have a higher burden of metabolic comorbidities and are more likely to develop a HFpEF phenotype, especially after menopause[255,258,290]. Although female patients with HFpEF have higher systemic and pulmonary vascular resistance and a lower systolic and diastolic reserve, with higher LV filling pressures during exercise[291], the rate of hospitalization for HF and cardiovascular and all-cause mortality are lower in female than in male patients across the LVEF spectrum[292]. In patients with isolated hypertension[293] and in rodents exposed to pressure overload[294,295], female individuals tend to develop concentric hypertrophy, whereas male individuals tend to develop eccentric hypertrophy with earlier progression into a HFrEF phenotype.

Multiple studies in premenopausal rodents have revealed that 17β-oestradiol (E2) protects females from cardiac hypertrophy and dysfunction through activation of oestrogen receptor-β (ERβ), but not ERα[295–299], which is associated with blunted activation of p38–mitogen-activated protein kinase[298], apoptotic cell death[295], and both redox-sensitive and ROS-sensitive events[154,300]. After ovariectomy (simulating menopause), this protection is largely lost but can be re-established by E2 administration[298]. The mechanisms by which E2 protects females from cardiac remodelling and dysfunction are multifaceted. E2 modulates mitochondrial function through genomic effects by activating ERα and ERβ to regulate transcription of peroxisome proliferator-activated receptor-γ coactivator 1α, nuclear respiratory factor 1 and mitochondrial transcription factor A that promote mitochondrial biogenesis and oxidative phosphorylation[301–303]. Furthermore, through non-genomic effects via membrane-bound receptors, such as ERβ localized directly on mitochondria[301,303–305], and also G protein-coupled oestrogen receptors, E2 initiates rapid signalling cascades that influence mitochondrial morphology, Ca^{2+} homeostasis and antioxidant defence mechanisms[301–303].

Of note, ROS production at the ETC and oxidative damage are lower in cardiac mitochondria from female compared with male rats[306,307]. This difference was traced to a higher efficiency of oxidative phosphorylation in female animals[306], governed by sex-dependent expression of mitochondrial cytochrome *c* oxidase subunit 7A2-like (COX7RP)[308], which is known to regulate ETC supercomplex assembly in an E2-sensitive manner in various cell types[309,310]. In young rats and humans, COX7RP expression is higher in female individuals than male individuals; with ageing in humans, or after ovariectomy in rats, COX7RP expression decreases in cardiac mitochondria of female individuals, reducing respiratory efficacy and increasing ROS formation, oxidizing RYR2 and provoking SR Ca^{2+} release, delayed afterdepolarizations and arrhythmias[308]. In addition, mitochondria from female rodents have lower rates of Ca^{2+} uptake[311], but higher Ca^{2+} accumulation capacity[312], which, together with the differences in ETC complex assembly and ROS production, protects against MPTP opening, providing cardioprotection after ischaemia–reperfusion in female animals[301,302,308].

Finally, E2 modulates mitochondrial quality control by attenuating mitophagy and fission via inhibition of dynamin-1-like protein and mitochondrial fission 1 protein, while promoting mitochondrial fusion, especially through effects on mitochondrial dynamin-like GTPase OPA1 and mitofusins, maintaining mitochondrial integrity and supporting cardiomyocyte survival under stress conditions, such as ischaemia–reperfusion injury and insulin resistance[301,302]. Taken together, these data indicate that, before menopause, E2 protects female individuals from mitochondrial dysfunction and ROS emission in various pathological conditions, including pathological mechanical workload.

In agreement with these data, the development of HFpEF in response to a high-fat diet plus L-NAME is blunted in young, premenopausal female mice[284,313]. However, in contrast to the observations in mice with pressure overload[295–299], ovariectomy did not abrogate this protection[313,314], suggesting that differences in HFpEF vulnerability might be unrelated to differences in E2 signalling. Alternatively, differences in inflammation, such as blunted expression of IL-6, IL-1β and inducible NO synthase, and a lack of activation of the X-box-binding protein 1 pathway were observed in female compared with male mice exposed to a high-fat diet and L-NAME[313]. Together, these and future data on sex-related and strain-dependent differences in mice might help to disentangle the precise mechanisms by which mechano-energetic uncoupling and its downstream consequences contribute to the development of HFpEF, not only in rodents but also in humans.

Disrupted NAD^+ metabolism as a treatable risk factor for HF?

Adequate availability of NAD^+ and NADH is crucial for the maintenance of myocardial bioenergetic efficiency and normal cardiac function[315]. NAD^+ deficiency not only impairs mitochondrial fatty acid β-oxidation and oxidative phosphorylation, but also deregulates various cellular processes, including nutrient sensing, DNA repair, epigenetic and post-translational regulation, autophagy and inflammatory signalling[315], all of which can independently contribute to the development of HF. Therefore, dysregulated NAD^+ homeostasis and redox imbalance (that is, an altered NADH:NAD^+ ratio) coincide with the pathogenesis of HF and its major risk factors, including obesity, hypertension and ageing[316–320].

Mounting preclinical evidence indicates that both prophylactic and therapeutic repletion of NAD^+ are beneficial in animal models of HFpEF and HFrEF. For example, supplementation with nicotinamide (NAM) improved diastolic dysfunction, LV hypertrophy and exercise intolerance in rat and mouse models of cardiometabolic HFpEF[317,321]. Similarly, nicotinamide riboside (NR) supplementation reversed cardiometabolic HFpEF in mice[318,319], and either NAM or NR supplementation reduced the risk of HFpEF in aged mice[317,320]. The cardioprotective mechanisms of NAD^+-based therapy against experimental HFpEF include improved mitochondrial function and myocardial bioenergetics and the deacetylation of titin and SERCA2a, which are key regulators of cardiomyocyte stiffness and relaxation, respectively[317,322]. In animal models of HFrEF, supplementation with NR[320,323] or the NAD^+ intermediate nicotinamide mononucleotide[316,324] protected against ventricular dilatation and dysfunction induced by transverse aortic constriction. NR supplementation also prevented ventricular dilatation and improved myocardial function in various genetic mouse models of DCM[323,325].

The cardioprotective effects of NR supplementation and the ensuing increase in NAD^+ levels in animal models of HFrEF were linked to improvements in NAD^+ redox balance and mitochondrial function, but were independent of sirtuin-mediated mitochondrial protein deacetylation[324], as initially proposed[316]. Of note, NR supplementation activated short-chain dehydrogenase/reductase enzymes, a family of NADP(H)-dependent and NAD(H)-dependent oxidoreductases, which mitigated the effects of HFrEF by stimulating retinoid signalling and restoring mitochondrial oxidative metabolism[324]. These alternative

cardioprotective mechanisms stimulated a coordinated increase in oxidative phosphorylation and fatty acid oxidation regardless of SIRT3-mediated mitochondrial protein deacetylation. Similarly, NAM supplementation induced autophagy and/or mitophagy independently of sirtuin-mediated deacetylation, corroborating the involvement of other mechanisms of action in NAD^+-targeted therapy[326]. Considering the cellular heterogeneity of the heart, experimental studies are needed to resolve the mechanisms underlying the mode of action of NAD^+ in a cell-type-specific manner and to elucidate potential sex-related differences in the efficacy of NAD^+ enhancers.

Taken together, robust preclinical evidence supports the role of dysregulated NAD^+ metabolism and the therapeutic potential of various NAD^+ precursors in combating HF across the spectrum of LVEF. Low cardiac NAD^+ and circulating NAM levels have also been measured in patients with HFpEF[317,319], supporting the rationale for using NAD^+ precursors as an adjunctive therapy. Similarly, in early phase trials, patients with DCM and HFrEF had cardiac NAD^+ deficiency[327], and the administration of NR had anti-inflammatory effects and improved mitochondrial respiration in peripheral blood mononuclear cells[328,329]. However, to investigate whether NAD^+ precursors also improve the clinical outcomes of patients with HF, larger phase II and phase III trials are required.

Clinical translation of targeting mechano-energetic (un)coupling in HF

Given the complexity of mechano-energetic uncoupling in HF, various treatment targets have emerged, including the mitochondria, metabolic substrate utilization, the sarcomeres and cytosolic ion handling. In this section, we outline the latest knowledge on treatments that target the pathomechanisms underlying mechano-energetic uncoupling in HF development. Using nomenclature suggested previously[330], we discriminate between compounds targeting intracellular substrate metabolism or mitochondria (so-called mitotropes) and compounds targeting the sarcomeres (so-called myotropes), largely comprising the group of cardiac myosin modulators. Current and future HF drugs[331], cardiac myosin modulators[29] and mechano-energetic aspects of inotropes[38] have been reviewed previously. An overview of clinical trials targeting mechano-energetic uncoupling in HF is provided in Table 1.

Mitotropes

More than 20 years ago[332], anti-anginal drugs (such as perhexiline, ranolazine and trimetazidine) that are used to alleviate symptoms in patients with ischaemic heart disease were proposed to improve cardiac efficiency by changing mitochondrial substrate utilization. These drugs reduce fatty acid metabolism through inhibition of mitochondrial fatty acid uptake, shifting metabolism to greater utilization of carbohydrates, and thereby have been suggested to improve energetic efficiency (that is, the ATP:O_2 ratio). Since then, various clinical studies have been performed to explore the clinical potential of these drugs in other forms of cardiac disease, such as chronic HF, DCM and HCM. In multiple trials, an improvement in peak O_2 consumption during exercise has been observed with these drugs[333,334]. However, the benefit of the proposed shift in substrate utilization is debated, and additional pleiotropic mechanisms such as a reduction in oxidative stress have been proposed[335], so these drugs remain under investigation. The latest example is ninerafaxstat, a competitive inhibitor of mitochondrial 3-ketoacyl-CoA thiolase (the last enzyme in the long-chain fatty acid β-oxidation pathway), which improved exercise capacity in patients with non-obstructive HCM[336,337].

As introduced above, elamipretide is a peptide compound that accumulates ~1,000-fold in mitochondria through its specific binding to cardiolipin[205,206]. The phase IIa EMBRACE STEMI study[338] in patients with acute ST-segment elevation myocardial infarction demonstrated the safety of elamipretide but reported no significant reduction in infarct size or improvement in LV function. Despite positive results in a large-animal model of ischaemic HFrEF[339] and confirmation of safety in patients with HFrEF[340], no improvement in LV geometry or function were observed in a subsequent phase II trial involving patients with HFrEF after (only) 4 weeks of treatment with elamipretide[341]. In 12 patients with Barth syndrome, treatment with elamipretide had no significant effects after 12 weeks of placebo-controlled treatment but improved LV stroke volume and several other functional parameters at 36 or 164 weeks in an open-label extension study that was completed by 8 patients[250,251]. Although relying on small numbers of patients with an orphan disease, these data suggest that longer-term treatment with elamipretide might be required to improve cardiac function or other clinical end points in patients with HF, which requires further investigation.

The Q-SYMBIO trial[342] evaluated treatment with CoQ_{10}, a component of the ETC that can act as an antioxidant and improve mitochondrial function. In 420 patients with HFrEF, CoQ_{10} treatment reduced major adverse cardiovascular events, suggesting potential benefits in the management of HF. Owing to the relatively small number of patients for a phase III outcome trial, the use of CoQ_{10} is not recommended in the European Society of Cardiology guidelines for the treatment of HF[343]. In a meta-analysis including 2,339 patients with HF treated with CoQ_{10}, a 36% reduction in all-cause mortality, a 50% reduction in hospitalization for HF and significant improvements in LVEF, New York Heart Association (NYHA) functional class and 6-min walking distance were observed[344]. However, large heterogeneity in patient numbers and trial designs limits the validity of the data[344] and warrants a larger prospective trial.

In a phase I trial, supplementation with NR with the aim of restoring cellular NAD^+ levels improved respiratory function in peripheral blood mononuclear cells and reduced inflammatory biomarkers in 30 patients with HFrEF[328]. Larger-scale trials are required to evaluate the effects of NR supplementation on cardiac parameters and outcomes.

Cardiac myosin modulators

Several trials have evaluated the use of mavacamten, a cardiac myosin inhibitor, in patients with obstructive HCM. In the EXPLORER-HCM trial[27], mavacamten reduced LVOT obstruction and plasma NT-proBNP and troponin T levels, and (as the primary end point) improved NYHA functional status and maximal O_2 uptake. Mavacamten has also been shown to improve quality of life in patients with obstructive HCM[345]. On the basis of these results, mavacamten was approved by the FDA and EMA and is widely used to treat obstructive HCM[346]. Aficamten, another cardiac myosin inhibitor, was evaluated in the SEQUOIA-HCM trial[28] and similarly reduced the LVOT gradient and plasma NT-proBNP and troponin T levels, and improved NYHA functional status and maximal O_2 uptake[28]. Aficamten has been submitted to the FDA and EMA for approval for the treatment of obstructive HCM.

Omecamtiv mecarbil is a cardiac myosin activator that prolongs the 'power stroke' during heart muscle contraction and thereby increases stroke volume[38]. This positive 'myotropic' effect increases cardiac output and lowers the endogenous sympathetic tone, which is why heart rate decreases slightly and cardiac O_2 consumption is not increased with omecamtiv mecarbil treatment[38]. In the GALACTIC-HF

Table 1 | Clinical trials of therapies targeting mechano-energetic uncoupling in HF

Therapeutic agent (trial name)	Patient cohort	Treatment	Primary end point	Results (all changes reported were significant)	Ref.
Mitotropes					
Ninerafaxstat	67 patients with non-obstructive HCM	200 mg twice daily for 12 weeks versus placebo	Safety and tolerability	Well tolerated, better exercise performance and health status in most symptomatically limited individuals	336
Elamipretide (phase I, NCT02388464)	36 patients with HFrEF	A single, 4-h infusion	Safety and efficacy up to 24 h after infusion	Safe and well tolerated; decreased LV end-diastolic volume	340
Elamipretide (phase II PROGRESS-HF)	71 patients with HFrEF	4 mg or 40 mg once daily by subcutaneous injection for 28 consecutive days	Change in LV end-systolic volume from baseline	No significant changes	341
Elamipretide (phase II TAZPower)	12 patients with Barth syndrome (10 entered open-label extension, 8 reached 168 weeks)	40 mg per day for a total of 28 weeks, followed by a 168-week open-label extension	Safety and tolerability (treatment-emergent adverse events, laboratory values, vital signs, physical examinations and electrocardiogram)	Overall safe and tolerated; adverse effects: injection-site reactions (80%) and pain (70%); secondary end points: improved LV stroke volume, end-diastolic and end-systolic volumes	251
Coenzyme Q_{10} (Q-SYMBIO)	420 patients with moderate to severe HF	100 mg three times daily for 2 years in addition to standard therapy	Short term (week 16): NYHA functional class, 6-min walking distance, plasma NT-proBNP level; long term (2 years): MACE	Short term: no significant difference; long term: 50% decrease in MACE, including a 43% reduction in cardiovascular mortality and a 49% reduction in all-cause mortality	342
Nicotinamide riboside (phase I, NCT03423342)	30 patients with HFrEF	1,000 mg twice daily for 12 weeks	Safety and tolerability; explorative end points: 6-min walking disease, mitochondrial function and expression of pro-inflammatory genes in peripheral blood mononuclear cells	Increased mitochondrial respiration and decreased pro-inflammatory cytokine expression in peripheral blood mononuclear cells	328
Cardiac myosin modulators					
Mavacamten (phase III EXPLORER-HCM)	251 patients with obstructive HCM	5 mg for 30 weeks	Improvement by ≥1.5 ml/kg/min in pVO_2 with improvement by ≥1 NYHA functional class, or improvement by ≥3.0 ml/kg/min in pVO_2 with no improvement in NYHA functional class	Improved exercise capacity, LVOT obstruction, NYHA functional class and health status	27
Mavacamten (phase III VALOR-HCM)	112 patients with obstructive HCM	5 mg daily, titrated up to 15 mg	Decision to proceed with SRT and SRT eligibility at week 16	Reduced the proportion of patients meeting guideline criteria for SRT	362
Mavacamten (phase III EXPLORER-CN)	81 patients with obstructive HCM from China	2.5 mg daily for 30 weeks	Change in post-Valsalva peak LVOT gradient after 30 weeks	Improved post-Valsalva LVOT gradient; all secondary efficacy end points also improved	363
Aficamten (phase III SEQUOIA-HCM)	282 patients with symptomatic obstructive HCM	5–20 mg for 24 weeks	Change in pVO_2 after 24 weeks	Improved pVO_2	28
Omecamtiv mecarbil (phase III GALACTIC-HF)	8,256 patients with HFrEF, LVEF ≤35%	25–50 mg twice daily for 21.8 months	First HF event (hospitalization or urgent visit for HF) or death from cardiovascular causes	8% reduction in the risk of a first HF event or cardiovascular death	26
Danicamtiv (phase IIa)	40 patients with HFrEF	50–100 mg twice daily for 7 days	Safety and tolerability of single and multiple oral doses	Improved LV systolic function and left atrial volume and function	348
SGLT2 inhibitors					
Empagliflozin (phase III EMPEROR-Reduced)	3,730 patients with HFrEF (class II–IV HF and LVEF ≤40%)	10 mg once daily in addition to recommended therapy	Composite of hospitalization for HF or cardiovascular death	25% reduction in the risk of hospitalization for HF or cardiovascular death	19
Empagliflozin (phase III EMPEROR-Preserved)	5,988 patients with HFpEF (LVEF ≥40%)	10 mg once daily in addition to usual therapy	Composite of hospitalization for HF or cardiovascular death	21% reduction in the risk of hospitalization for HF or cardiovascular death	17
Dapagliflozin (phase III DAPA-HF)	4,744 patients with HFrEF (LVEF ≤40%)	10 mg once daily in addition to recommended therapy	Composite of worsening HF or cardiovascular death	26% reduction in the risk of worsening HF or cardiovascular death	18

Table 1 (continued) | Clinical trials of therapies targeting mechano-energetic uncoupling in HF

Therapeutic agent (trial name)	Patient cohort	Treatment	Primary end point	Results (all changes reported were significant)	Ref.
SGLT2 inhibitors (continued)					
Dapagliflozin (phase III, DELIVER)	6,263 patients with HFpEF (LVEF ≥40%)	10 mg once daily in addition to usual therapy for 2.3 years	Composite of worsening HF or cardiovascular death	18% reduction in the risk of worsening HF or cardiovascular death	20
GLP1-based treatments					
Semaglutide (phase III, STEP-HFpEF)	529 patients with HFpEF and obesity (BMI ≥30) but without diabetes	Semaglutide (2.4 mg) or placebo once weekly for 52 weeks	Change in KCCQ-CSS and body weight	Increase in KCCQ-CSS by 7.8 points and reduction in body weight by 10.7% (estimated differences versus placebo)	23
Semaglutide (phase III, STEP-HFpEF DM)	616 patients with HFpEF with obesity (BMI ≥30) and diabetes	Semaglutide (2.4 mg) or placebo once weekly for 52 weeks	Change in KCCQ-CSS and body weight	Increase in KCCQ-CSS by 7.3 points and reduction in body weight by 6.4% (estimated differences versus placebo)	24
Tirzepatide (phase III, SUMMIT)	713 patients with HFpEF and obesity (BMI ≥30) with or without diabetes	Tirzepatide (15 mg) or placebo once weekly for at least 52 weeks	Composite of adjudicated cardiovascular death or worsening HF event and change in KCCQ-CSS	38% reduction in cardiovascular death or worsening HF; between-group difference in KCCQ-CSS of +6.9 points	22

GLP1, glucagon-like peptide 1; HCM, hypertrophic cardiomyopathy; HF, heart failure; HFpEF, heart failure with preserved ejection fraction; HFrEF, heart failure with reduced ejection fraction; KCCQ-CSS, Kansas City Cardiomyopathy Questionnaire clinical summary score (scores range from 0 to 100, with higher scores indicating better quality of life); LV, left ventricular; LVEF, left ventricular ejection fraction; LVOT, left ventricular outflow tract; MACE, major adverse cardiovascular events; NYHA, New York Heart Association; pVO_2, peak oxygen uptake; SGLT2, sodium–glucose cotransporter 2; SRT, septal reduction therapy.

study[26], omecamtiv mecarbil was tested in >8,000 patients with HFrEF (25% hospitalized at enrolment). The primary end point of hospitalization for HF or cardiovascular mortality was reduced by 8% with omecamtiv mecarbil treatment compared with placebo, whereas the individual components of the end point were not significantly reduced. A subgroup analysis showed that the more severely ill patients (those who were hospitalized with high plasma NT-proBNP levels and/or had a LVEF of <28%) particularly benefited from omecamtiv mecarbil treatment[347]. Interestingly, omecamtiv mecarbil worked best in patients in sinus rhythm and not as well in those with atrial fibrillation or flutter[26]. A possible explanation for this observation was provided by a smaller study involving the cardiac myosin activator danicamtiv, which improved not only the LV stroke volume but also the left atrial function index in patients with HFrEF[348]. Therefore, in addition to prolonging the systolic ejection time of the left ventricle, cardiac myosin activators might also improve LV filling by increasing the atrial 'kick', which presumably compensates for the slightly shortened LV filling time due to prolongation of the systolic ejection time. Despite the positive results and the potential to target treatment with cardiac myosin activators to patients with HFrEF with low LVEF, who are hospitalized and/or who have high plasma NT-proBNP levels, the FDA has not yet approved omecamtiv mecarbil for the treatment of HFrEF. To confirm the positive results of omecamtiv mecarbil in patients with HFrEF, lower LVEF and higher plasma NT-proBNP levels[26,347], the phase III COMET-HF trial[349] is ongoing in patients with HFrEF, a LVEF of <30% and a plasma NT-proBNP level of ≥1,000 pg/ml. The effects of omecamtiv mecarbil and other inotropes on cardiac mechano-energetic coupling have been reviewed in detail previously[38].

Compounds targeting systemic metabolism

SGLT2 inhibitors such as dapagliflozin and empagliflozin were developed (and are approved) for the treatment of diabetes, but have also been shown to reduce hospitalization for HF and cardiovascular mortality in patients with HF, irrespective of LVEF and of the presence of diabetes[17–20]. The underlying mechanisms are not fully resolved. The observation that patients benefit irrespective of the presence of diabetes suggests the existence of off-target (and SGLT2-independent) effects, which is supported by preclinical studies on *Sglt2*-knockout mice[350,351]. Several other studies reported that SGLT2 inhibitors lower $[Na^+]_i$ in cardiomyocytes, by inhibiting NHE[350,352,353], $I_{Na,L}$ and/or CaMKII (refs. 354–356), which also increased mitochondrial Ca^{2+} accumulation[352]. Dapagliflozin and empagliflozin are approved and recommended for use in patients with HF across the entire spectrum of LVEF[343,357] and also those with chronic kidney disease[358], reflecting their broad and systemic benefits beyond blood glucose control.

In patients with HFpEF and obesity, the GLP1 receptor agonist semaglutide reduced body weight, improved quality of life and lowered plasma NT-proBNP and C-reactive protein concentrations[23,24]. In a meta-analysis, semaglutide reduced the combined end point of hospitalization for HF and cardiovascular mortality in patients with obesity and HFpEF, driven largely by the reduction in hospitalization[21]. Tirzepatide, a combined GLP1 receptor and glucose-dependent insulinotropic polypeptide (GIP) receptor agonist, is more efficient than semaglutide in reducing body weight in patients with obesity[359], but mediated similar effects as those of semaglutide in patients with HFpEF and obesity[22]. Interestingly, the tirzepatide-associated improvements in symptoms and quality of life in patients with HFpEF and obesity closely correlate with the reductions in blood volume and blood pressure, suggesting that haemodynamic and mechano-energetic changes might have an important role in these benefits[360]. In agreement with this hypothesis, tirzepatide treatment also reduces myocardial mass[361].

Conclusions

Mechano-energetic uncoupling is a central element in the pathophysiology of both HFrEF and HFpEF (Figs. 3 and 4). In HFrEF, cardiac damage is often the initiating event that triggers neuroendocrine activation, which then alters EC coupling and impairs mitochondrial Ca^{2+} handling (Fig. 3). By contrast, HFpEF is often initiated by non-cardiac

comorbidities, such as obesity and hypertension, which impose elevated preload and afterload on the heart and, consequently, increased metabolic demand that is not sufficiently matched by mitochondrial adaptations (Fig. 3). By the reverse mode of NNT, this energetic mismatch is translated into oxidative stress, which can activate a number of redox-sensitive kinases, including CaMKII, a central molecular hub that mediates hypercontractility, but also maladaptive cardiac hypertrophy and remodelling and, if excessive, also cell death (Figs. 1, 3 and 4). Hereditary cardiomyopathies, such as HCM or Barth syndrome, show pathophysiological similarities to the acquired forms of HF, and involve disrupted metabolic demand or supply, respectively (Figs. 3–5). A deeper knowledge of the intricate interaction between cardiac mechanics and energetics will help to understand the efficacy of current HF therapies and aid the development of novel tools to interrupt the vicious cycle of mechano-energetic uncoupling that drives cardiac remodelling and dysfunction in various aetiologies of HF (Fig. 4 and Table 1).

Published online: 22 June 2025

References

1. Bozkurt, B. et al. HF STATS 2024: heart failure epidemiology and outcomes statistics an updated 2024 report from the Heart Failure Society of America. *J. Card. Fail.* https://doi.org/10.1016/j.cardfail.2024.07.001 (2024).
2. Ng, M. et al. Global, regional, and national prevalence of overweight and obesity in children and adults during 1980–2013: a systematic analysis for the global burden of disease study 2013. *Lancet* **384**, 766–781 (2014).
3. Maack, C. et al. Heart failure and diabetes: metabolic alterations and therapeutic interventions: a state-of-the-art review from the translational research committee of the Heart Failure Association–European Society of Cardiology. *Eur. Heart J.* **39**, 4243–4254 (2018).
4. Braunwald, E. Diabetes, heart failure, and renal dysfunction: the vicious circles. *Prog. Cardiovasc. Dis.* **62**, 298–302 (2019).
5. Robertson, J. et al. Body mass index in young women and risk of cardiomyopathy: a long-term follow-up study in Sweden. *Circulation* **141**, 520–529 (2020).
6. Robertson, J. et al. Higher body mass index in adolescence predicts cardiomyopathy risk in midlife. *Circulation* **140**, 117–125 (2019).
7. Setoguchi, S., Stevenson, L. W. & Schneeweiss, S. Repeated hospitalizations predict mortality in the community population with heart failure. *Am. Heart J.* **154**, 260–266 (2007).
8. Mamas, M. A. et al. Do patients have worse outcomes in heart failure than in cancer? A primary care-based cohort study with 10-year follow-up in Scotland. *Eur. J. Heart Fail.* **19**, 1095–1104 (2017).
9. Murashige, D. et al. Comprehensive quantification of fuel use by the failing and nonfailing human heart. *Science* **370**, 364–368 (2020).
10. Neubauer, S. et al. Myocardial phosphocreatine-to-ATP ratio is a predictor of mortality in patients with dilated cardiomyopathy. *Circulation* **96**, 2190–2196 (1997).
11. Phan, T. T. et al. Heart failure with preserved ejection fraction is characterized by dynamic impairment of active relaxation and contraction of the left ventricle on exercise and associated with myocardial energy deficiency. *J. Am. Coll. Cardiol.* **54**, 402–409 (2009).
12. Mahmod, M. et al. The interplay between metabolic alterations, diastolic strain rate and exercise capacity in mild heart failure with preserved ejection fraction: a cardiovascular magnetic resonance study. *J. Cardiovasc. Magn. Reson.* **20**, 88 (2018).
13. Neubauer, S. The failing heart — an engine out of fuel. *N. Engl. J. Med.* **356**, 1140–1151 (2007).
14. Bertero, E. & Maack, C. Metabolic remodelling in heart failure. *Nat. Rev. Cardiol.* **15**, 457–470 (2018).
15. Bertero, E. & Maack, C. Calcium signaling and reactive oxygen species in mitochondria. *Circ. Res.* **122**, 1460–1478 (2018).
16. Ardehali, H. et al. Targeting myocardial substrate metabolism in heart failure: potential for new therapies. *Eur. J. Heart Fail.* **14**, 120–129 (2012).
17. Anker, S. D. et al. Empagliflozin in heart failure with a preserved ejection fraction. *N. Engl. J. Med.* **385**, 1451–1461 (2021).
18. McMurray, J. J. V. et al. Dapagliflozin in patients with heart failure and reduced ejection fraction. *N. Engl. J. Med.* **381**, 1995–2008 (2019).
19. Packer, M. et al. Cardiovascular and renal outcomes with empagliflozin in heart failure. *N. Engl. J. Med.* **383**, 1413–1424 (2020).
20. Solomon, S. D. et al. Dapagliflozin in heart failure with mildly reduced or preserved ejection fraction. *N. Engl. J. Med.* **387**, 1089–1098 (2022).
21. Kosiborod, M. N. et al. Semaglutide versus placebo in patients with heart failure and mildly reduced or preserved ejection fraction: a pooled analysis of the SELECT, FLOW, STEP-HFpEF, and STEP-HFpEF DM randomised trials. *Lancet* **404**, 949–961 (2024).
22. Packer, M. et al. Tirzepatide for heart failure with preserved ejection fraction and obesity. *N. Engl. J. Med.* **392**, 427–437 (2025).
23. Kosiborod, M. N. et al. Semaglutide in patients with heart failure with preserved ejection fraction and obesity. *N. Engl. J. Med.* **389**, 1069–1084 (2023).
24. Kosiborod, M. N. et al. Semaglutide in patients with obesity-related heart failure and type 2 diabetes. *N. Engl. J. Med.* **390**, 1394–1407 (2024).
25. Böhm, M., Bewarder, Y. & Kindermann, I. Ejection fraction in heart failure revisited- where does the evidence start? *Eur. Heart J.* **41**, 2363–2365 (2020).
26. Teerlink, J. R. et al. Cardiac myosin activation with omecamtiv mecarbil in systolic heart failure. *N. Engl. J. Med.* **384**, 105–116 (2021).
27. Olivotto, I. et al. Mavacamten for treatment of symptomatic obstructive hypertrophic cardiomyopathy (EXPLORER-HCM): a randomised, double-blind, placebo-controlled, phase 3 trial. *Lancet* **396**, 759–769 (2020).
28. Maron, M. S. et al. Aficamten for symptomatic obstructive hypertrophic cardiomyopathy. *N. Engl. J. Med.* **390**, 1849–1861 (2024).
29. Lehman, S. J., Crocini, C. & Leinwand, L. A. Targeting the sarcomere in inherited cardiomyopathies. *Nat. Rev. Cardiol.* **19**, 353–363 (2022).
30. Saks, V. et al. Cardiac system bioenergetics: metabolic basis of the Frank–Starling law. *J. Physiol.* **571**, 253–273 (2006).
31. Bers, D. M. Cardiac excitation-contraction coupling. *Nature* **415**, 198–205 (2002).
32. Schramm, M., Klieber, H. G. & Daut, J. The energy expenditure of actomyosin-ATPase, Ca(2+)-ATPase and Na+,K(+)-ATPase in guinea-pig cardiac ventricular muscle. *J. Physiol.* **481**, 647–662 (1994).
33. Balaban, R. S., Nemoto, S. & Finkel, T. Mitochondria, oxidants, and aging. *Cell* **120**, 483–495 (2005).
34. Nickel, A., Kohlhaas, M. & Maack, C. Mitochondrial reactive oxygen species production and elimination. *J. Mol. Cell. Cardiol.* **73C**, 26–33 (2014).
35. Aon, M. A., Cortassa, S. & O'Rourke, B. Redox-optimized ROS balance: a unifying hypothesis. *Biochim. Biophys. Acta* **1797**, 865–877 (2010).
36. Cortassa, S., O'Rourke, B. & Aon, M. A. Redox-optimized ROS balance and the relationship between mitochondrial respiration and ROS. *Biochim. Biophys. Acta* **1837**, 287–295 (2014).
37. Puglisi, J. L., Negroni, J. A., Chen-Izu, Y. & Bers, D. M. The force–frequency relationship: insights from mathematical modeling. *Adv. Physiol. Educ.* **37**, 28–34 (2013).
38. Maack, C. et al. Treatments targeting inotropy. *Eur. Heart J.* **40**, 3626–3644 (2019).
39. Kaur, S., Shen, X., Power, A. & Ward, M. L. Stretch modulation of cardiac contractility: importance of myocyte calcium during the slow force response. *Biophys. Rev.* **12**, 135–142 (2020).
40. Sequeira, V., Maack, C., Reil, G. H. & Reil, J. C. Exploring the connection between relaxed myosin states and the anrep effect. *Circ. Res.* **134**, 117–134 (2024).
41. Chen-Izu, Y., Banyasz, T., Shaw, J. A. & Izu, L. T. The heart is a smart pump: mechanotransduction mechanisms of the frank-starling law and the anrep effect. *Annu. Rev. Physiol.* **87**, 53–77 (2025).
42. Brandes, R. & Bers, D. M. Intracellular Ca^{2+} increases the mitochondrial NADH concentration during elevated work in intact cardiac muscle. *Circ. Res.* **80**, 82–87 (1997).
43. Cortassa, S., Aon, M. A., Marbán, E., Winslow, R. L. & O'Rourke, B. An integrated model of cardiac mitochondrial energy metabolism and calcium dynamics. *Biophys. J.* **84**, 2734–2755 (2003).
44. Maack, C. et al. Elevated cytosolic Na^+ decreases mitochondrial Ca^{2+} uptake during excitation–contraction coupling and impairs energetic adaptation in cardiac myocytes. *Circ. Res.* **99**, 172–182 (2006).
45. Maack, C. & O'Rourke, B. Excitation–contraction coupling and mitochondrial energetics. *Basic Res. Cardiol.* **102**, 369–392 (2007).
46. McCormack, J. G., Halestrap, A. P. & Denton, R. M. Role of calcium ions in regulation of mammalian intramitochondrial metabolism. *Physiol. Rev.* **70**, 391–425 (1990).
47. Territo, P. R., French, S. A., Dunleavy, M. C., Evans, F. J. & Balaban, R. S. Calcium activation of heart mitochondrial oxidative phosphorylation: rapid kinetics of mVO_2, NADH, and light scattering. *J. Biol. Chem.* **276**, 2586–2599 (2001).
48. Balaban, R. S. Cardiac energy metabolism homeostasis: role of cytosolic calcium. *J. Mol. Cell. Cardiol.* **34**, 1259–1271 (2002).
49. Luongo, T. S. et al. The mitochondrial calcium uniporter matches energetic supply with cardiac workload during stress and modulates permeability transition. *Cell Rep.* **12**, 23–34 (2015).
50. Kohlhaas, M. et al. Elevated cytosolic Na^+ increases mitochondrial formation of reactive oxygen species in failing cardiac myocytes. *Circulation* **121**, 1606–1613 (2010).
51. Rizzuto, R. & Pozzan, T. Microdomains of intracellular Ca^{2+}: molecular determinants and functional consequences. *Physiol. Rev.* **86**, 369–408 (2006).
52. Lu, X. et al. Measuring local gradients of intramitochondrial $[Ca^{2+}]$ in cardiac myocytes during sarcoplasmic reticulum Ca(2+) release. *Circ. Res.* **112**, 424–431 (2013).
53. Kohlhaas, M. & Maack, C. Adverse bioenergetic consequences of Na^+–Ca^{2+} exchanger-mediated Ca^{2+} influx in cardiac myocytes. *Circulation* **122**, 2273–2280 (2010).
54. Williams, G. S., Boyman, L., Chikando, A. C., Khairallah, R. J. & Lederer, W. J. Mitochondrial calcium uptake. *Proc. Natl Acad. Sci. USA* **110**, 10479–10486 (2013).
55. Mackenzie, L., Roderick, H. L., Berridge, M. J., Conway, S. J. & Bootman, M. D. The spatial pattern of atrial cardiomyocyte calcium signalling modulates contraction. *J. Cell Sci.* **117**, 6327–6337 (2004).
56. Ljubojevic, S. et al. Early remodeling of perinuclear Ca^{2+} stores and nucleoplasmic Ca^{2+} signaling during the development of hypertrophy and heart failure. *Circulation* **130**, 244–255 (2014).
57. Voglhuber, J. et al. Functional remodelling of perinuclear mitochondria alters nucleoplasmic Ca^{2+} signalling in heart failure. *Philos. Trans. R. Soc. Lond. B* **377**, 20210320 (2022).

58. Rosencrans, W. M., Aguilella, V. M., Rostovtseva, T. K. & Bezrukov, S. M. α-Synuclein emerges as a potent regulator of VDAC-facilitated calcium transport. *Cell Calcium* **95**, 102355 (2021).
59. Baradaran, R., Wang, C., Siliciano, A. F. & Long, S. B. Cryo-EM structures of fungal and metazoan mitochondrial calcium uniporters. *Nature* **559**, 580–584 (2018).
60. Baughman, J. M. et al. Integrative genomics identifies MCU as an essential component of the mitochondrial calcium uniporter. *Nature* **476**, 341–345 (2011).
61. Bick, A. G., Calvo, S. E. & Mootha, V. K. Evolutionary diversity of the mitochondrial calcium uniporter. *Science* **336**, 886 (2012).
62. De Stefani, D., Raffaello, A., Teardo, E., Szabo, I. & Rizzuto, R. A forty-kilodalton protein of the inner membrane is the mitochondrial calcium uniporter. *Nature* **476**, 336–340 (2011).
63. Sancak, Y. et al. EMRE is an essential component of the mitochondrial calcium uniporter complex. *Science* **342**, 1379–1382 (2013).
64. Payne, R., Li, C. & Foskett, J. K. Variable assembly of EMRE and MCU creates functional channels with distinct gatekeeping profiles. *iScience* **23**, 101037 (2020).
65. Watanabe, A. et al. Quantitative analysis of mitochondrial calcium uniporter (MCU) and essential MCU regulator (EMRE) in mitochondria from mouse tissues and HeLa cells. *FEBS Open Bio* **12**, 811–826 (2022).
66. Perocchi, F. et al. MICU1 encodes a mitochondrial EF hand protein required for Ca^{2+} uptake. *Nature* **467**, 291–296 (2010).
67. Csordas, G. et al. MICU1 controls both the threshold and cooperative activation of the mitochondrial Ca^{2+} uniporter. *Cell Metab.* **17**, 976–987 (2013).
68. Tsai, C. W. et al. Mechanisms and significance of tissue-specific MICU regulation of the mitochondrial calcium uniporter complex. *Mol. Cell* **82**, 3661–3676 e3668 (2022).
69. Plovanich, M. et al. MICU2, a paralog of MICU1, resides within the mitochondrial uniporter complex to regulate calcium handling. *PLoS ONE* **8**, e55785 (2013).
70. Patron, M., Granatiero, V., Espino, J., Rizzuto, R. & De Stefani, D. MICU3 is a tissue-specific enhancer of mitochondrial calcium uptake. *Cell Death Differ.* **26**, 179–195 (2019).
71. Kamer, K. J., Jiang, W., Kaushik, V. K., Mootha, V. K. & Grabarek, Z. Crystal structure of MICU2 and comparison with MICU1 reveal insights into the uniporter gating mechanism. *Proc. Natl Acad. Sci. USA* **116**, 3546–3555 (2019).
72. Paillard, M. et al. Tissue-specific mitochondrial decoding of cytoplasmic Ca2$^+$ signals is controlled by the stoichiometry of MICU1/2 and MCU. *Cell Rep.* **18**, 2291–2300 (2017).
73. Patron, M. et al. MICU1 and MICU2 finely tune the mitochondrial Ca^{2+} uniporter by exerting opposite effects on MCU activity. *Mol. Cell* **53**, 726–737 (2014).
74. Xing, Y. et al. Dimerization of MICU proteins controls Ca^{2+} influx through the mitochondrial Ca^{2+} uniporter. *Cell Rep.* **26**, 1203–1212 e1204 (2019).
75. Lambert, J. P. et al. MCUB regulates the molecular composition of the mitochondrial calcium uniporter channel to limit mitochondrial calcium overload during stress. *Circulation* **140**, 1720–1733 (2019).
76. Raffaello, A. et al. The mitochondrial calcium uniporter is a multimer that can include a dominant-negative pore-forming subunit. *EMBO J.* **32**, 2362–2376 (2013).
77. Fieni, F., Lee, S. B., Jan, Y. N. & Kirichok, Y. Activity of the mitochondrial calcium uniporter varies greatly between tissues. *Nat. Commun.* **3**, 1317 (2012).
78. Berridge, M. J. Cardiac calcium signalling. *Biochem. Soc. Trans.* **31**, 930–933 (2003).
79. Tomar, D. & Elrod, J. W. Metabolite regulation of the mitochondrial calcium uniporter channel. *Cell Calcium* **92**, 102288 (2020).
80. Kwong, J. Q. et al. The mitochondrial calcium uniporter selectively matches metabolic output to acute contractile stress in the heart. *Cell Rep.* **12**, 15–22 (2015).
81. Gunter, T. E. & Pfeiffer, D. R. Mechanisms by which mitochondria transport calcium. *Am. J. Physiol.* **258**, C755–C786 (1990).
82. Kirichok, Y., Krapivinsky, G. & Clapham, D. E. The mitochondrial calcium uniporter is a highly selective ion channel. *Nature* **427**, 360–364 (2004).
83. De La Fuente, S. et al. Strategic positioning and biased activity of the mitochondrial calcium uniporter in cardiac muscle. *J. Biol. Chem.* **291**, 23343–23362 (2016).
84. Kohlhaas, M. & Maack, C. Calcium release microdomains and mitochondria. *Cardiovasc. Res.* **98**, 259–268 (2013).
85. Giacomello, M. & Pellegrini, L. The coming of age of the mitochondria–ER contact: a matter of thickness. *Cell Death Differ.* **23**, 1417–1427 (2016).
86. Peskoff, A. & Langer, G. A. Calcium concentration and movement in the ventricular cardiac cell during an excitation–contraction cycle. *Biophys. J.* **74**, 153–174 (1998).
87. Seidlmayer, L. K. et al. Inositol 1,4,5-trisphosphate-mediated sarcoplasmic reticulum-mitochondrial crosstalk influences adenosine triphosphate production via mitochondrial Ca^{2+} uptake through the mitochondrial ryanodine receptor in cardiac myocytes. *Cardiovasc. Res.* **112**, 491–501 (2016).
88. Wu, S. et al. Binding of FUN14 domain containing 1 with inositol 1,4,5-trisphosphate receptor in mitochondria-associated endoplasmic reticulum membranes maintains mitochondrial dynamics and function in hearts in vivo. *Circulation* **136**, 2248–2266 (2017).
89. Chen, Y. et al. Mitofusin 2-containing mitochondrial-reticular microdomains direct rapid cardiomyocyte bioenergetic responses via interorganelle Ca^{2+} crosstalk. *Circ. Res.* **111**, 863–875 (2012).
90. Aksentijevic, D. & Shattock, M. J. With a grain of salt: sodium elevation and metabolic remodelling in heart failure. *J. Mol. Cell. Cardiol.* **161**, 106–115 (2021).
91. Aksentijevic, D., O'Brien, B. A., Eykyn, T. R. & Shattock, M. J. Is there a causal link between intracellular Na elevation and metabolic remodelling in cardiac hypertrophy? *Biochem. Soc. Trans.* **46**, 817–827 (2018).
92. Pieske, B. & Houser, S. R. [Na$^+$]i handling in the failing human heart. *Cardiovasc. Res.* **57**, 874–886 (2003).
93. Shattock, M. J. & Bers, D. M. Rat vs. rabbit ventricle: Ca flux and intracellular Na assessed by ion-selective microelectrodes. *Am. J. Physiol.* **256**, C813–C822 (1989).
94. Fuller, W. et al. Regulation of the cardiac sodium pump. *Cell Mol. Life Sci.* **70**, 1357–1380 (2013).
95. Cross, H. R., Radda, G. K. & Clarke, K. The role of Na^+/K^+ ATPase activity during low flow ischemia in preventing myocardial injury: a 31P, 23Na and 87Rb NMR spectroscopic study. *Magn. Reson. Med.* **34**, 673–685 (1995).
96. Okamoto, K., Wang, W., Rounds, J., Chambers, E. A. & Jacobs, D. O. ATP from glycolysis is required for normal sodium homeostasis in resting fast-twitch rodent skeletal muscle. *Am. J. Physiol. Endocrinol. Metab.* **281**, E479–E488 (2001).
97. Ingwall, J. S. On the control of metabolic remodeling in mitochondria of the failing heart. *Circ. Heart Fail.* **2**, 275–277 (2009).
98. Bessman, S. P. & Carpenter, C. L. The creatine–creatine phosphate energy shuttle. *Annu. Rev. Biochem.* **54**, 831–862 (1985).
99. Lygate, C. A. Maintaining energy provision in the heart: the creatine kinase system in ischaemia–reperfusion injury and chronic heart failure. *Clin. Sci.* **138**, 491–514 (2024).
100. Winkler, C. et al. Estimation of left ventricular stroke work based on a large cohort of healthy children. *Comput. Biol. Med.* **123**, 103908 (2020).
101. Lygate, C. A. & Neubauer, S. in *Cardiac Energy Metabolism in Health and Disease* (eds G. D. Lopaschuk & N. S. Dhalla) 155–168 (Springer, 2014).
102. Dzeja, P. & Terzic, A. Adenylate kinase and AMP signaling networks: metabolic monitoring, signal communication and body energy sensing. *Int. J. Mol. Sci.* **10**, 1729–1772 (2009).
103. Bers, D. M. Altered cardiac myocyte Ca regulation in heart failure. *Physiology* **21**, 380–387 (2006).
104. O'Rourke, B. et al. Mechanisms of altered excitation–contraction coupling in canine tachycardia-induced heart failure, I: experimental studies. *Circ. Res.* **84**, 562–570 (1999).
105. Maltsev, V. A. et al. Novel, ultraslow inactivating sodium current in human ventricular cardiomyocytes. *Circulation* **98**, 2545–2552 (1998).
106. Despa, S., Islam, M. A., Weber, C. R., Pogwizd, S. M. & Bers, D. M. Intracellular Na^+ concentration is elevated in heart failure but Na/K pump function is unchanged. *Circulation* **105**, 2543–2548 (2002).
107. Yokoyama, H., Gunasegaram, S., Harding, S. E. & Avkiran, M. Sarcolemmal Na^+/H^+ exchanger activity and expression in human ventricular myocardium. *J. Am. Coll. Cardiol.* **36**, 534–540 (2000).
108. Baartscheer, A. et al. Increased Na^+/H^+-exchange activity is the cause of increased [Na^+]i and underlies disturbed calcium handling in the rabbit pressure and volume overload heart failure model. *Cardiovasc. Res.* **57**, 1015–1024 (2003).
109. Bay, J., Kohlhaas, M. & Maack, C. Intracellular Na^+ and cardiac metabolism. *J. Mol. Cell. Cardiol.* **61**, 20–27 (2013).
110. Armoundas, A. A., Hobai, I. A., Tomaselli, G. F., Winslow, R. L. & O'Rourke, B. Role of sodium–calcium exchanger in modulating the action potential of ventricular myocytes from normal and failing hearts. *Circ. Res.* **93**, 46–53 (2003).
111. Weber, C. R., Piacentino, V. 3rd, Houser, S. R. & Bers, D. M. Dynamic regulation of sodium/calcium exchange function in human heart failure. *Circulation* **108**, 2224–2229 (2003).
112. Weisser-Thomas, J., Piacentino, V. 3rd, Gaughan, J. P., Margulies, K. & Houser, S. R. Calcium entry via Na/Ca exchange during the action potential directly contributes to contraction of failing human ventricular myocytes. *Cardiovasc. Res.* **57**, 974–985 (2003).
113. Sipido, K. R., Maes, M. & Van de Werf, F. Low efficiency of Ca^{2+} entry through the Na^+–Ca^{2+} exchanger as trigger for Ca^{2+} release from the sarcoplasmic reticulum. A comparison between L-type Ca^{2+} current and reverse-mode Na^+–Ca^{2+} exchange. *Circ. Res.* **81**, 1034–1044 (1997).
114. Michels, G. et al. Regulation of the human cardiac mitochondrial Ca^{2+} uptake by 2 different voltage-gated Ca^{2+} channels. *Circulation* **119**, 2435–2443 (2009).
115. Luongo, T. S. et al. The mitochondrial Na^+/Ca^{2+} exchanger is essential for Ca^{2+} homeostasis and viability. *Nature* **545**, 93–97 (2017).
116. Paillard, M. et al. Altered composition of the mitochondrial Ca^{2+}uniporter in the failing human heart. *Cell Calcium* **105**, 102618 (2022).
117. Pinali, C., Bennett, H., Davenport, J. B., Trafford, A. W. & Kitmitto, A. Three-dimensional reconstruction of cardiac sarcoplasmic reticulum reveals a continuous network linking transverse-tubules: this organization is perturbed in heart failure. *Circ. Res.* **113**, 1219–1230 (2013).
118. Goh, K. Y. et al. Impaired mitochondrial network excitability in failing guinea-pig cardiomyocytes. *Cardiovasc. Res.* **109**, 79–89 (2016).
119. Maack, C. Orphaned mitochondria in heart failure. *Cardiovasc. Res.* **109**, 6–8 (2016).
120. Chen, Y. & Dorn, G. W. 2nd. PINK1-phosphorylated mitofusin 2 is a Parkin receptor for culling damaged mitochondria. *Science* **340**, 471–475 (2013).
121. Van Steenbergen, V. et al. Nano-positioning and tubulin conformation contribute to axonal transport regulation of mitochondria along microtubules. *Proc. Natl Acad. Sci. USA* **119**, e2203499119 (2022).
122. Chen, C. Y. et al. Suppression of detyrosinated microtubules improves cardiomyocyte function in human heart failure. *Nat. Med.* **24**, 1225–1233 (2018).
123. Kuznetsov, A. V. et al. Mitochondrial subpopulations and heterogeneity revealed by confocal imaging: possible physiological role? *Biochim. Biophys. Acta* **1757**, 686–691 (2006).
124. Meyer, M. et al. Frequency-dependence of myocardial energetics in failing human myocardium as quantified by a new method for the measurement of oxygen consumption in muscle strip preparations. *J. Mol. Cell. Cardiol.* **30**, 1459–1470 (1998).

125. Liu, T. & O'Rourke, B. Enhancing mitochondrial Ca^{2+} uptake in myocytes from failing hearts restores energy supply and demand matching. *Circ. Res.* **103**, 279–288 (2008).
126. Erickson, J. R. et al. A dynamic pathway for calcium-independent activation of CaMKII by methionine oxidation. *Cell* **133**, 462–474 (2008).
127. Ago, T. et al. A redox-dependent pathway for regulating class II HDACs and cardiac hypertrophy. *Cell* **133**, 978–993 (2008).
128. Weissman, D. & Maack, C. Redox signaling in heart failure and therapeutic implications. *Free Radic. Biol. Med.* **171**, 345–364 (2021).
129. Aksentijevic, D. et al. Intracellular sodium elevation reprograms cardiac metabolism. *Nat. Commun.* **11**, 4337 (2020).
130. Chung, Y. J. et al. Elevated Na is a dynamic and reversible modulator of mitochondrial metabolism in the heart. *Nat. Commun.* **15**, 4277 (2024).
131. Liu, T., Brown, D. A. & O'Rourke, B. Role of mitochondrial dysfunction in cardiac glycoside toxicity. *J. Mol. Cell. Cardiol.* **49**, 728–736 (2010).
132. Hernansanz-Agustín, P. et al. Na^+ controls hypoxic signalling by the mitochondrial respiratory chain. *Nature* **586**, 287–291 (2020).
133. Liu, T. et al. Inhibiting mitochondrial Na^+/Ca^{2+} exchange prevents sudden death in a guinea pig model of heart failure. *Circ. Res.* **115**, 44–54 (2014).
134. Liu, T., Yang, N., Sidor, A. & O'Rourke, B. MCU overexpression rescues inotropy and reverses heart failure by reducing SR Ca^{2+} leak. *Circ. Res.* **128**, 1191–1204 (2021).
135. Fossier, L. et al. Enhanced mitochondrial calcium uptake suppresses atrial fibrillation associated with metabolic syndrome. *J. Am. Coll. Cardiol.* **80**, 2205–2219 (2022).
136. Dey, S., DeMazumder, D., Sidor, A., Foster, D. B. & O'Rourke, B. Mitochondrial ROS drive sudden cardiac death and chronic proteome remodeling in heart failure. *Circ. Res.* **123**, 356–371 (2018).
137. Hegyi, B. et al. Cardiomyocyte Na^+ and Ca^{2+} mishandling drives vicious cycle involving CaMKII, ROS, and ryanodine receptors. *Basic Res. Cardiol.* **116**, 58 (2021).
138. Bertero, E., Popoiu, T. A. & Maack, C. Mitochondrial calcium in cardiac ischemia/reperfusion injury and cardioprotection. *Basic Res. Cardiol.* **119**, 569–585 (2024).
139. Murphy, E. & Eisner, D. A. How does mitochondrial Ca^{2+} change during ischemia and reperfusion? Implications for activation of the permeability transition pore. *J. Gen. Physiol.* **157**, e202313520 (2025).
140. Halestrap, A. Biochemistry: a pore way to die. *Nature* **434**, 578–579 (2005).
141. Zhou, B. & Tian, R. Mitochondrial dysfunction in pathophysiology of heart failure. *J. Clin. Invest.* **128**, 3716–3726 (2018).
142. Nakayama, H. et al. Ca^{2+}- and mitochondrial-dependent cardiomyocyte necrosis as a primary mediator of heart failure. *J. Clin. Invest.* **117**, 2431–2444 (2007).
143. Sommakia, S. et al. Mitochondrial cardiomyopathies feature increased uptake and diminished efflux of mitochondrial calcium. *J. Mol. Cell. Cardiol.* **113**, 22–32 (2017).
144. Santulli, G., Xie, W., Reiken, S. R. & Marks, A. R. Mitochondrial calcium overload is a key determinant in heart failure. *Proc. Natl Acad. Sci. USA* **112**, 11389–11394 (2015).
145. Desai, K. H. et al. Cardiovascular indexes in the mouse at rest and with exercise: new tools to study models of cardiac disease. *Am. J. Physiol.* **272**, H1053–H1061 (1997).
146. Georgakopoulos, D. & Kass, D. Minimal force–frequency modulation of inotropy and relaxation of in situ murine heart. *J. Physiol.* **534**, 535–545 (2001).
147. Chapman, C. B., Fisher, J. N. & Sproule, B. J. Behavior of stroke volume at rest and during exercise in human beings. *J. Clin. Invest.* **39**, 1208–1213 (1960).
148. Grimby, G., Nilsson, N. J. & Saltin, B. Cardiac output during submaximal and maximal exercise in active middle-aged athletes. *J. Appl. Physiol.* **21**, 1150–1156 (1966).
149. Pan, X. et al. The physiological role of mitochondrial calcium revealed by mice lacking the mitochondrial calcium uniporter. *Nat. Cell Biol.* **15**, 1464–1472 (2013).
150. Cox, D. A. & Matlib, M. A. A role for the mitochondrial Na^+–Ca^{2+} exchanger in the regulation of oxidative phosphorylation in isolated heart mitochondria. *J. Biol. Chem.* **268**, 938–947 (1993).
151. Elrod, J. W. et al. Cyclophilin D controls mitochondrial pore-dependent Ca^{2+} exchange, metabolic flexibility, and propensity for heart failure in mice. *J. Clin. Invest.* **120**, 3680–3687 (2010).
152. O'Rourke, B., Ashok, D. & Liu, T. Mitochondrial Ca^{2+} in heart failure: not enough or too much? *J. Mol. Cell. Cardiol.* **151**, 126–134 (2021).
153. Phillips, D. et al. Regulation of oxidative phosphorylation complex activity: effects of tissue-specific metabolic stress within an allometric series and acute changes in workload. *Am. J. Physiol. Regul. Integr. Comp. Physiol.* **302**, R1034–R1048 (2012).
154. Nickel, A. G. et al. Reversal of mitochondrial transhydrogenase causes oxidative stress in heart failure. *Cell Metab.* **22**, 472–484 (2015).
155. Garcia-Menendez, L., Karamanlidis, G., Kolwicz, S. & Tian, R. Substrain specific response to cardiac pressure overload in C57BL/6 mice. *Am. J. Physiol. Heart Circ. Physiol.* **305**, H397–H402 (2013).
156. Müller, M. et al. Right heart failure in mice upon pressure overload is promoted by mitochondrial oxidative stress. *JACC Basic Transl. Sci.* **7**, 658–677 (2022).
157. Reil, J. C. et al. CaMKII activity contributes to homeometric autoregulation of the heart: a novel mechanism for the Anrep effect. *J. Physiol.* **598**, 3129–3153 (2020).
158. Wang, W. et al. Sustained β1-adrenergic stimulation modulates cardiac contractility by Ca^{2+}/calmodulin kinase signaling pathway. *Circ. Res.* **95**, 798–806 (2004).
159. Reyes Gaido, O. E. et al. CaMKII as a therapeutic target in cardiovascular disease. *Annu. Rev. Pharmacol. Toxicol.* **63**, 249–272 (2023).
160. Morbach, C. et al. Heart rate-corrected systolic ejection time: population-based reference values and differential prognostic utility in acute heart failure. *Eur. Heart J.* **1**, qyad020 (2023).
161. Herrmann, G. & Decherd, G. The chemical nature of heart failure. *Ann. Intern. Med.* **12**, 1233–1244 (1939).
162. Gabr, R. E. et al. Cardiac work is related to creatine kinase energy supply in human heart failure: a cardiovascular magnetic resonance spectroscopy study. *J. Cardiovasc. Magn. Reson.* **20**, 81 (2018).
163. Weiss, R. G., Gerstenblith, G. & Bottomley, P. A. ATP flux through creatine kinase in the normal, stressed, and failing human heart. *Proc. Natl Acad. Sci. USA* **102**, 808–813 (2005).
164. Ye, Y., Gong, G., Ochiai, K., Liu, J. & Zhang, J. High-energy phosphate metabolism and creatine kinase in failing hearts: a new porcine model. *Circulation* **103**, 1570–1576 (2001).
165. Shen, W. et al. The fall in creatine levels and creatine kinase isozyme changes in the failing heart are reversible: complex post-transcriptional regulation of the components of the CK system. *J. Mol. Cell. Cardiol.* **39**, 537–544 (2005).
166. Shen, W., Vatner, D. E., Vatner, S. F. & Ingwall, J. S. Progressive loss of creatine maintains a near normal $\Delta G_{\sim ATP}$ in transgenic mouse hearts with cardiomyopathy caused by overexpressing Gsα. *J. Mol. Cell. Cardiol.* **48**, 591–599 (2010).
167. Sequeira, V. et al. Synergistic role of ADP and Ca^{2+} in diastolic myocardial stiffness. *J. Physiol.* **593**, 3899–3916 (2015).
168. Tian, R., Nascimben, L., Ingwall, J. S. & Lorell, B. H. Failure to maintain a low ADP concentration impairs diastolic function in hypertrophied rat hearts. *Circulation* **96**, 1313–1319 (1997).
169. Dzeja, P. P., Vitkevicius, K. T., Redfield, M. M., Burnett, J. C. & Terzic, A. Adenylate kinase-catalyzed phosphotransfer in the myocardium : increased contribution in heart failure. *Circ. Res.* **84**, 1137–1143 (1999).
170. Aksentijevic, D. et al. High-energy phosphotransfer in the failing mouse heart: role of adenylate kinase and glycolytic enzymes. *Eur. J. Heart Fail.* **12**, 1282–1289 (2010).
171. Ten Hove, M. et al. Mechanisms of creatine depletion in chronically failing rat heart. *J. Mol. Cell. Cardiol.* **38**, 309–313 (2005).
172. Neubauer, S. et al. Downregulation of the Na^+–creatine cotransporter in failing human myocardium and in experimental heart failure. *Circulation* **100**, 1847–1850 (1999).
173. Heinke, M. Y. et al. Changes in myocardial protein expression in pacing-induced canine heart failure. *Electrophoresis* **20**, 2086–2093 (1999).
174. Marín-García, J., Goldenthal, M. J., Damle, S., Pi, Y. & Moe, G. W. Regional distribution of mitochondrial dysfunction and apoptotic remodeling in pacing-induced heart failure. *J. Card. Fail.* **15**, 700–708 (2009).
175. Walker, M. A. et al. Acetylation of muscle creatine kinase negatively impacts high-energy phosphotransfer in heart failure. *JCI Insight* **6**, e144301 (2021).
176. Park, S. J. et al. Myocardial creatine kinase expression after left ventricular assist device support. *J. Am. Coll. Cardiol.* **39**, 1773–1779 (2002).
177. Lygate, C. A. et al. Living without creatine: unchanged exercise capacity and response to chronic myocardial infarction in creatine-deficient mice. *Circ. Res.* **112**, 945–955 (2013).
178. Arbelo, E. et al. 2023 ESC Guidelines for the management of cardiomyopathies: developed by the task force on the management of cardiomyopathies of the European Society of Cardiology (ESC). *Eur. Heart J.* **44**, 3503–3626 (2023).
179. Watkins, H., Ashrafian, H. & Redwood, C. Inherited cardiomyopathies. *N. Engl. J. Med.* **364**, 1643–1656 (2011).
180. Authors/Task Force Members 2014 ESC Guidelines on diagnosis and management of hypertrophic cardiomyopathy: the task force for the diagnosis and management of hypertrophic cardiomyopathy of the European Society of Cardiology (ESC). *Eur. Heart J.* **35**, 2733–2779 (2014).
181. Semsarian, C., Ingles, J., Maron, M. S. & Maron, B. J. New perspectives on the prevalence of hypertrophic cardiomyopathy. *J. Am. Coll. Cardiol.* **65**, 1249–1254 (2015).
182. Frey, N., Luedde, M. & Katus, H. A. Mechanisms of disease: hypertrophic cardiomyopathy. *Nat. Rev. Cardiol.* **9**, 91–100 (2012).
183. Ommen, S. R. et al. 2024 AHA/ACC/AMSSM/HRS/PACES/SCMR guideline for the management of hypertrophic cardiomyopathy. *J. Am. Coll. Cardiol.* **83**, 2324–2405 (2024).
184. Finocchiaro, G., Westaby, J., Sheppard, M. N., Papadakis, M. & Sharma, S. Sudden cardiac death in young athletes: JACC state-of-the-art review. *J. Am. Coll. Cardiol.* **83**, 350–370 (2024).
185. Geisterfer-Lowrance, A. A. et al. A molecular basis for familial hypertrophic cardiomyopathy: a β cardiac myosin heavy chain gene missense mutation. *Cell* **62**, 999–1006 (1990).
186. Bonne, G. et al. Cardiac myosin binding protein-C gene splice acceptor site mutation is associated with familial hypertrophic cardiomyopathy. *Nat. Genet.* **11**, 438–440 (1995).
187. Watkins, H. et al. Mutations in the genes for cardiac troponin T and α-tropomyosin in hypertrophic cardiomyopathy. *N. Engl. J. Med.* **332**, 1058–1064 (1995).
188. Ho, C. Y. et al. Assessment of diastolic function with doppler tissue imaging to predict genotype in preclinical hypertrophic cardiomyopathy. *Circulation* **105**, 2992–2997 (2002).
189. Belus, A. et al. The familial hypertrophic cardiomyopathy-associated myosin mutation R403Q accelerates tension generation and relaxation of human cardiac myofibrils. *J. Physiol.* **586**, 3639–3644 (2008).
190. Witjas-Paalberends, E. R. et al. Gene-specific increase in the energetic cost of contraction in hypertrophic cardiomyopathy caused by thick filament mutations. *Cardiovasc. Res.* **103**, 248–257 (2014).
191. De Roos, A. et al. Cardiac metabolism in patients with dilated and hypertrophic cardio-myopathy: assessment with proton-decoupled P-31 MR spectroscopy. *J. Magn. Reson. Imaging* **2**, 711–719 (1992).

192. Sieverding, L. et al. Proton-decoupled myocardial 31P NMR spectroscopy reveals decreased PCr/Pi in patients with severe hypertrophic cardiomyopathy. *Am. J. Cardiol.* **80**, 34A–40A (1997).
193. Jung, W.-I. et al. P NMR spectroscopy detects metabolic abnormalities in asymptomatic patients with hypertrophic cardiomyopathy. *Circulation* **97**, 2536–2542 (1998).
194. Crilley, J. G. et al. Hypertrophic cardiomyopathy due to sarcomeric gene mutations is characterized by impaired energy metabolism irrespective of the degree of hypertrophy. *J. Am. Coll. Cardiol.* **41**, 1776–1782 (2003).
195. Jung, W.-I. et al. Differences in cardiac energetics between patients with familial and nonfamilial hypertrophic cardiomyopathy. *Circulation* **101**, e121–e121 (2000).
196. Dass, S. et al. Exacerbation of cardiac energetic impairment during exercise in hypertrophic cardiomyopathy: a potential mechanism for diastolic dysfunction. *Eur. Heart J.* **36**, 1547–1554 (2015).
197. Spindler, M. et al. Diastolic dysfunction and altered energetics in the αMHC403/+ mouse model of familial hypertrophic cardiomyopathy. *J. Clin. Invest.* **101**, 1775–1783 (1998).
198. Ranjbarvaziri, S. et al. Altered cardiac energetics and mitochondrial dysfunction in hypertrophic cardiomyopathy. *Circulation* **144**, 1714–1731 (2021).
199. Previs, M. J. et al. Defects in the proteome and metabolome in human hypertrophic cardiomyopathy. *Circ. Heart Fail.* **15**, e009521 (2022).
200. Wang, W. et al. Metabolic characterization of hypertrophic cardiomyopathy in human heart. *Nat. Cardiovasc. Res.* **1**, 445–461 (2022).
201. Moore, J. et al. Multi-omics profiling of hypertrophic cardiomyopathy reveals altered mechanisms in mitochondrial dynamics and excitation-contraction coupling. *Int. J. Mol. Sci.* **24**, 4724 (2023).
202. Nollet, E. E. et al. Mitochondrial dysfunction in human hypertrophic cardiomyopathy is linked to cardiomyocyte architecture disruption and corrected by improving NADH-driven mitochondrial respiration. *Eur. Heart J.* **44**, 1170–1185 (2023).
203. Kohlhaas, M. et al. Mitochondrial reactive oxygen species cause arrhythmias in hypertrophic cardiomyopathy. Preprint at *bioRxiv* https://doi.org/10.1101/2024.10.02.616214 (2024).
204. Huke, S. et al. Focal energy deprivation underlies arrhythmia susceptibility in mice with calcium-sensitized myofilaments. *Circ. Res.* **112**, 1334–1344 (2013).
205. Brown, D. A. et al. Mitochondrial function as a therapeutic target in heart failure. *Nat. Rev. Cardiol.* **14**, 238–250 (2017).
206. Szeto, H. H. First-in-class cardiolipin-protective compound as a therapeutic agent to restore mitochondrial bioenergetics. *Br. J. Pharmacol.* **171**, 2029–2050 (2014).
207. Coppini, R. et al. Late sodium current inhibition reverses electromechanical dysfunction in human hypertrophic cardiomyopathy. *Circulation* **127**, 575–584 (2013).
208. Helms, A. S. et al. Genotype-dependent and -independent calcium signaling dysregulation in human hypertrophic cardiomyopathy. *Circulation* **134**, 1738–1748 (2016).
209. Lehman, S. J. et al. Chronic calmodulin-kinase II activation drives disease progression in mutation-specific hypertrophic cardiomyopathy. *Circulation* **139**, 1517–1529 (2019).
210. Robinson, P. et al. Hypertrophic cardiomyopathy mutations increase myofilament Ca^{2+} buffering, alter intracellular Ca^{2+} handling, and stimulate Ca^{2+}-dependent signaling. *J. Biol. Chem.* **293**, 10487–10499 (2018).
211. Okuda, S. et al. CaMKII-mediated phosphorylation of RyR2 plays a crucial role in aberrant Ca^{2+} release as an arrhythmogenic substrate in cardiac troponin T-related familial hypertrophic cardiomyopathy. *Biochem. Biophys. Res. Commun.* **496**, 1250–1256 (2018).
212. Wagner, S. et al. Ca^{2+}/calmodulin-dependent protein kinase II regulates cardiac Na^{+} channels. *J. Clin. Invest.* **116**, 3127–3138 (2006).
213. Backs, J., Song, K., Bezprozvannaya, S., Chang, S. & Olson, E. N. CaM kinase II selectively signals to histone deacetylase 4 during cardiomyocyte hypertrophy. *J. Clin. Invest.* **116**, 1853–1864 (2006).
214. Kuster, G. M. et al. α-Adrenergic receptor-stimulated hypertrophy in adult rat ventricular myocytes is mediated via thioredoxin-1-sensitive oxidative modification of thiols on Ras. *Circulation* **111**, 1192–1198 (2005).
215. Niemeyer, C. M. RAS diseases in children. *Haematologica* **99**, 1653–1662 (2014).
216. Wu, X. et al. MEK-ERK pathway modulation ameliorates disease phenotypes in a mouse model of Noonan syndrome associated with the *Raf1*^{L613V} mutation. *J. Clin. Invest.* **121**, 1009–1025 (2011).
217. Wilder, T., Ryba, D. M., Wieczorek, D. F., Wolska, B. M. & Solaro, R. J. *N*-Acetylcysteine reverses diastolic dysfunction and hypertrophy in familial hypertrophic cardiomyopathy. *Am. J. Physiol.* **309**, H1720–H1730 (2015).
218. Lombardi, R. et al. Resolution of established cardiac hypertrophy and fibrosis and prevention of systolic dysfunction in a transgenic rabbit model of human cardiomyopathy through thiol-sensitive mechanisms. *Circulation* **119**, 1398–1407 (2009).
219. Marian, A. J., Senthil, V., Chen, S. N. & Lombardi, R. Antifibrotic effects of antioxidant *N*-acetylcysteine in a mouse model of human hypertrophic cardiomyopathy mutation. *J. Am. Coll. Cardiol.* **47**, 827–834 (2006).
220. Kehat, I. et al. Extracellular signal-regulated kinases 1 and 2 regulate the balance between eccentric and concentric cardiac growth. *Circ. Res.* **108**, 176–183 (2011).
221. Davis, J. et al. A tension-based model distinguishes hypertrophic versus dilated cardiomyopathy. *Cell* **165**, 1147–1159 (2016).
222. Dai, D. F. et al. Mitochondrial targeted antioxidant peptide ameliorates hypertensive cardiomyopathy. *J. Am. Coll. Cardiol.* **58**, 73–82 (2011).
223. Dai, D. F. et al. Mitochondrial oxidative stress mediates angiotensin II-induced cardiac hypertrophy and Gαq overexpression-induced heart failure. *Circ. Res.* **108**, 837–846 (2011).
224. Batzner, A., Schäfers, H.-J., Borisov, K. V. & Seggewiß, H. Hypertrophic obstructive cardiomyopathy. *Dtsch. Arztebl Int.* **116**, 47–53 (2019).
225. Maron, M. S. et al. Effect of left ventricular outflow tract obstruction on clinical outcome in hypertrophic cardiomyopathy. *N. Engl. J. Med.* **348**, 295–303 (2003).
226. Sigwart, U. Non-surgical myocardial reduction for hypertrophic obstructive cardiomyopathy. *Lancet* **346**, 211–214 (1995).
227. Green, E. M. et al. A small-molecule inhibitor of sarcomere contractility suppresses hypertrophic cardiomyopathy in mice. *Science* **351**, 617–621 (2016).
228. Hegde, S. M. et al. Effect of mavacamten on echocardiographic features in symptomatic patients with obstructive hypertrophic cardiomyopathy. *J. Am. Coll. Cardiol.* **78**, 2518–2532 (2021).
229. Saberi, S. et al. Mavacamten favorably impacts cardiac structure in obstructive hypertrophic cardiomyopathy. *Circulation* **143**, 606–608 (2021).
230. Lee, M. M. Y. et al. Aficamten and cardiopulmonary exercise test performance: a substudy of the SEQUOIA-HCM randomized clinical trial. *JAMA Cardiol.* **9**, 990–1000 (2024).
231. Masri, A. et al. Effect of aficamten on cardiac structure and function in obstructive hypertrophic cardiomyopathy: SEQUOIA-HCM CMR substudy. *J. Am. Coll. Cardiol.* **84**, 1806–1817 (2024).
232. Dudek, J. & Maack, C. Mechano-energetic aspects of Barth syndrome. *J. Inherit. Metab. Dis.* **45**, 82–98 (2022).
233. Barth, P. G. et al. An X-linked mitochondrial disease affecting cardiac muscle, skeletal muscle and neutrophil leucocytes. *J. Neurol. Sci.* **62**, 327–355 (1983).
234. Chowdhury, S. et al. Longitudinal observational study of cardiac outcome risk factor prediction in children, adolescents, and adults with barth syndrome. *Pediatr. Cardiol.* **43**, 1251–1263 (2022).
235. Spencer, C. T. et al. Impaired cardiac reserve and severely diminished skeletal muscle O_2 utilization mediate exercise intolerance in Barth syndrome. *Am. J. Physiol.* **301**, H2122–H2129 (2011).
236. Spencer, C. T. et al. Ventricular arrhythmia in the X-linked cardiomyopathy Barth syndrome. *Pediatr. Cardiol.* **26**, 632–637 (2005).
237. Wang, G. et al. Modeling the mitochondrial cardiomyopathy of Barth syndrome with induced pluripotent stem cell and heart-on-chip technologies. *Nat. Med.* **20**, 616–623 (2014).
238. Dudek, J. et al. Cardiolipin deficiency affects respiratory chain function and organization in an induced pluripotent stem cell model of Barth syndrome. *Stem Cell Res.* **11**, 806–819 (2013).
239. Wang, S. et al. AAV gene therapy prevents and reverses heart failure in a murine knockout model of barth syndrome. *Circ. Res.* **126**, 1024–1039 (2020).
240. Liu, X. et al. Increased reactive oxygen species-mediated Ca^{2+}/calmodulin-dependent protein kinase II activation contributes to calcium handling abnormalities and impaired contraction in Barth syndrome. *Circulation* **143**, 1894–1911 (2021).
241. Bertero, E. et al. Loss of mitochondrial Ca^{2+} uniporter limits inotropic reserve and provides trigger and substrate for arrhythmias in Barth syndrome cardiomyopathy. *Circulation* **144**, 1694–1713 (2021).
242. Ghosh, S. et al. An essential role for cardiolipin in the stability and function of the mitochondrial calcium uniporter. *Proc. Natl Acad. Sci. USA* **117**, 16383–16390 (2020).
243. Ghosh, S. et al. MCU-complex-mediated mitochondrial calcium signaling is impaired in Barth syndrome. *Hum. Mol. Genet.* **31**, 376–385 (2022).
244. Goncalves, R. L. S., Schlame, M., Bartelt, A., Brand, M. D. & Hotamışlıgil, G. S. Cardiolipin deficiency in Barth syndrome is not associated with increased superoxide/H_2O_2 production in heart and skeletal muscle mitochondria. *FEBS Lett.* **595**, 415–432 (2021).
245. Kutschka, I. et al. Activation of the integrated stress response rewires cardiac metabolism in Barth syndrome. *Basic Res. Cardiol.* **118**, 47 (2023).
246. Thompson, R. et al. Current and future treatment approaches for Barth syndrome. *J. Inherit. Metab. Dis.* **45**, 17–28 (2022).
247. Suzuki-Hatano, S. et al. AAV-mediated TAZ gene replacement restores mitochondrial and cardioskeletal function in Barth syndrome. *Hum. Gene. Ther.* **30**, 139–154 (2019).
248. Russo, S., De Rasmo, D., Rossi, R., Signorile, A. & Lobasso, S. SS-31 treatment ameliorates cardiac mitochondrial morphology and defective mitophagy in a murine model of Barth syndrome. *Sci. Rep.* **14**, 13655 (2024).
249. Russo, S., De Rasmo, D., Signorile, A., Corcelli, A. & Lobasso, S. Beneficial effects of SS-31 peptide on cardiac mitochondrial dysfunction in tafazzin knockdown mice. *Sci. Rep.* **12**, 19847 (2022).
250. Reid Thompson, W. et al. A phase 2/3 randomized clinical trial followed by an open-label extension to evaluate the effectiveness of elamipretide in Barth syndrome, a genetic disorder of mitochondrial cardiolipin metabolism. *Genet. Med.* **23**, 471–478 (2021).
251. Thompson, W. R. et al. Long-term efficacy and safety of elamipretide in patients with Barth syndrome: 168-week open-label extension results of TAZPOWER. *Genet. Med.* **26**, 101138 (2024).
252. Owan, T. E. et al. Trends in prevalence and outcome of heart failure with preserved ejection fraction. *N. Engl. J. Med.* **355**, 251–259 (2006).
253. Groenewegen, A., Rutten, F. H., Mosterd, A. & Hoes, A. W. Epidemiology of heart failure. *Eur. J. Heart Fail.* **22**, 1342–1356 (2020).
254. Cannata, A. & McDonagh, T. A. Heart failure with preserved ejection fraction. *N. Engl. J. Med.* **392**, 173–184 (2025).
255. Lam, C. S. P. et al. Sex differences in heart failure. *Eur. Heart J.* **40**, 3859–3868c (2019).
256. Bhatia, R. S. et al. Outcome of heart failure with preserved ejection fraction in a population-based study. *N. Engl. J. Med.* **355**, 260–269 (2006).
257. Streng, K. W. et al. Non-cardiac comorbidities in heart failure with reduced, mid-range and preserved ejection fraction. *Int. J. Cardiol.* **271**, 132–139 (2018).

258. Butler, J. et al. Effect of empagliflozin in patients with heart failure across the spectrum of left ventricular ejection fraction. *Eur. Heart J.* **43**, 416–426 (2022).
259. Kraigher-Krainer, E. et al. Impaired systolic function by strain imaging in heart failure with preserved ejection fraction. *J. Am. Coll. Cardiol.* **63**, 447–456 (2014).
260. Cikes, M. & Solomon, S. D. Beyond ejection fraction: an integrative approach for assessment of cardiac structure and function in heart failure. *Eur. Heart J.* **37**, 1642–1650 (2016).
261. Borlaug, B. A. Evaluation and management of heart failure with preserved ejection fraction. *Nat. Rev. Cardiol.* https://doi.org/10.1038/s41569-020-0363-2 (2020).
262. Pieske, B. et al. How to diagnose heart failure with preserved ejection fraction: the HFA-PEFF diagnostic algorithm: a consensus recommendation from the Heart Failure Association (HFA) of the European Society of Cardiology (ESC). *Eur. J. Heart Fail.* **22**, 391–412 (2020).
263. Bristow, M. R. Treatment of chronic heart failure with β-adrenergic receptor antagonists: a convergence of receptor pharmacology and clinical cardiology. *Circ. Res.* **109**, 1176–1194 (2011).
264. Rosch, S. et al. Characteristics of heart failure with preserved ejection fraction across the range of left ventricular ejection fraction. *Circulation* **146**, 506–518 (2022).
265. Jones, E. et al. Phenotyping heart failure using model-based analysis and physiology-informed machine learning. *J. Physiol.* **599**, 4991–5013 (2021).
266. Almeida-Coelho, J. et al. Myosin-inhibitor mavacamten acutely enhances cardiomyocyte diastolic compliance in heart failure with preserved ejection fraction. *Circ. Heart Fail.* **17**, e011833 (2024).
267. Aslam, M. I. et al. Reduced right ventricular sarcomere contractility in heart failure with preserved ejection fraction and severe obesity. *Circulation* **143**, 965–967 (2021).
268. Shah, S. J. et al. Cardiac myosin inhibition in heart failure with normal and supranormal ejection fraction: primary results of the EMBARK-HFpEF trial. *JAMA Cardiol.* **10**, 170–175 (2025).
269. Trum, M. et al. Empagliflozin inhibits increased Na influx in atrial cardiomyocytes of patients with HFpEF. *Cardiovasc. Res.* **120**, 999–1010 (2024).
270. Mira Hernandez, J. et al. Differential sex-dependent susceptibility to diastolic dysfunction and arrhythmia in cardiomyocytes from obese diabetic HFpEF model. *Cardiovasc. Res.* https://doi.org/10.1093/cvr/cvae070 (2024).
271. Yoshii, A. et al. Blunted cardiac mitophagy in response to metabolic stress contributes to HFpEF. *Circ. Res.* **135**, 1004–1017 (2024).
272. AbouEzzeddine, O. F. et al. Myocardial energetics in heart failure with preserved ejection fraction. *Circ. Heart Fail.* **12**, e006240 (2019).
273. Pandey, A. et al. Relationship between physical activity, body mass index, and risk of heart failure. *J. Am. Coll. Cardiol.* **69**, 1129–1142 (2017).
274. Adamson, C. et al. Dapagliflozin for heart failure according to body mass index: the DELIVER trial. *Eur. Heart J.* **43**, 4406–4417 (2022).
275. Ehrhart-Bornstein, M. et al. Human adipocytes secrete mineralocorticoid-releasing factors. *Proc. Natl Acad. Sci. USA* **100**, 14211–14216 (2003).
276. Huby, A.-C. et al. Adipocyte-derived hormone leptin is a direct regulator of aldosterone secretion, which promotes endothelial dysfunction and cardiac fibrosis. *Circulation* **132**, 2134–2145 (2015).
277. Packer, M. Leptin-aldosterone-neprilysin axis. *Circulation* **137**, 1614–1631 (2018).
278. Di Bello, V. et al. Obesity cardiomyopathy: is it a reality? An ultrasonic tissue characterization study. *J. Am. Soc. Echocardiogr.* **19**, 1063–1071 (2006).
279. Obokata, M., Reddy, Y. N. V., Pislaru, S. V., Melenovsky, V. & Borlaug, B. A. Evidence supporting the existence of a distinct obese phenotype of heart failure with preserved ejection fraction. *Circulation* **136**, 6–19 (2017).
280. Litwin, S. E. et al. Obesity in heart failure with preserved ejection fraction: insights from the REDUCE LAP-HF II trial. *Eur. J. Heart Fail.* **26**, 177–189 (2024).
281. Meddeb, M. et al. Myocardial ultrastructure of human heart failure with preserved ejection fraction. *Nat. Cardiovasc. Res.* **3**, 907–914 (2024).
282. Lourenço, A. P. et al. An integrative translational approach to study heart failure with preserved ejection fraction: a position paper from the Working Group on Myocardial Function of the European Society of Cardiology. *Eur. J. Heart Fail.* **20**, 216–227 (2018).
283. Schiattarella, G. G. et al. Nitrosative stress drives heart failure with preserved ejection fraction. *Nature* **568**, 351–356 (2019).
284. Pepin, M.E. et al. Mitochondrial NNT promotes diastolic dysfunction in cardiometabolic HFpEF. *Circ. Res.* https://doi.org/10.1161/CIRCRESAHA.125.326154 (2025).
285. Dia, M. et al. Reduced reticulum-mitochondria Ca^{2+} transfer is an early and reversible trigger of mitochondrial dysfunctions in diabetic cardiomyopathy. *Basic Res. Cardiol.* **115**, 74 (2020).
286. Hamilton, S. et al. MCU overexpression evokes disparate dose-dependent effects on mito-ROS and spontaneous Ca^{2+} release in hypertrophic rat cardiomyocytes. *Am. J. Physiol.* **321**, H615–H632 (2021).
287. Cherpaz, M. et al. Myocardial transcriptomic analysis of diabetic patients with aortic stenosis: key role for mitochondrial calcium signaling. *Cardiovasc. Diabetol.* **23**, 239 (2024).
288. Miranda-Silva, D. et al. Disturbed cardiac mitochondrial and cytosolic calcium handling in a metabolic risk-related rat model of heart failure with preserved ejection fraction. *Acta Physiol.* **228**, e13378 (2020).
289. Chyou, J. Y., Qin, H., Butler, J., Voors, A. A. & Lam, C. S. P. Sex-related similarities and differences in responses to heart failure therapies. *Nat. Rev. Cardiol.* **21**, 498–516 (2024).
290. Bergan, N. et al. Systematic review, meta-analysis, and population study to determine the biologic sex ratio in dilated cardiomyopathy. *Circulation* **151**, 442–459 (2025).
291. Beale, A. L. et al. Sex differences in heart failure with preserved ejection fraction pathophysiology: a detailed invasive hemodynamic and echocardiographic analysis. *JACC Heart Fail.* **7**, 239–249 (2019).
292. Qiu, W. et al. Sex differences in long-term heart failure prognosis: a comprehensive meta-analysis. *Eur. J. Prev. Cardiol.* **31**, 2013–2023 (2024).
293. Krumholz, H. M., Larson, M. & Levy, D. Sex differences in cardiac adaptation to isolated systolic hypertension. *Am. J. Cardiol.* **72**, 310–313 (1993).
294. Douglas, P. S. et al. Hypertrophic remodeling: gender differences in the early response to left ventricular pressure overload. *J. Am. Coll. Cardiol.* **32**, 1118–1125 (1998).
295. Fliegner, D. et al. Female sex and estrogen receptor-β attenuate cardiac remodeling and apoptosis in pressure overload. *Am. J. Physiol.* **298**, R1597–R1606 (2010).
296. Skavdahl, M. et al. Estrogen receptor-β mediates male-female differences in the development of pressure overload hypertrophy. *Am. J. Physiol.* **288**, H469–H476 (2005).
297. Patten, R. D. et al. 17 Beta-estradiol differentially affects left ventricular and cardiomyocyte hypertrophy following myocardial infarction and pressure overload. *J. Card. Fail.* **14**, 245–253 (2008).
298. van Eickels, M. et al. 17β-Estradiol attenuates the development of pressure-overload hypertrophy. *Circulation* **104**, 1419–1423 (2001).
299. Babiker, F. A. et al. Estrogen receptor β protects the murine heart against left ventricular hypertrophy. *Arterioscler. Thromb. Vasc. Biol.* **26**, 1524–1530 (2006).
300. Clerk, A., Fuller, S. J., Michael, A. & Sugden, P. H. Stimulation of 'stress-regulated' mitogen-activated protein kinases (stress-activated protein kinases/c-Jun N-terminal kinases and p38-mitogen-activated protein kinases) in perfused rat hearts by oxidative and other stresses. *J. Biol. Chem.* **273**, 7228–7234 (1998).
301. Ventura-Clapier, R., Piquereau, J., Veksler, V. & Garnier, A. Estrogens, estrogen receptors effects on cardiac and skeletal muscle mitochondria. *Front. Endocrinol.* **10**, 557 (2019).
302. Beikoghli Kalkhoran, S. & Kararigas, G. Oestrogenic regulation of mitochondrial dynamics. *Int. J. Mol. Sci.* **23**, 1118 (2022).
303. Klinge, C. M. Estrogens regulate life and death in mitochondria. *J. Bioenerg. Biomembr.* **49**, 307–324 (2017).
304. Simpkins, J. W., Yang, S.-H., Sarkar, S. N. & Pearce, V. Estrogen actions on mitochondria — physiological and pathological implications. *Mol. Cell. Endocrinol.* **290**, 51–59 (2008).
305. Yang, S.-H. et al. Mitochondrial localization of estrogen receptor β. *Proc. Natl Acad. Sci. USA* **101**, 4130–4135 (2004).
306. Colom, B., Oliver, J., Roca, P. & Garcia-Palmer, F. J. Caloric restriction and gender modulate cardiac muscle mitochondrial H_2O_2 production and oxidative damage. *Cardiovasc. Res.* **74**, 456–465 (2007).
307. Khalifa, A. R. et al. Sex-specific differences in mitochondria biogenesis, morphology, respiratory function, and ROS homeostasis in young mouse heart and brain. *Physiol. Rep.* **5**, e13125 (2017).
308. Clements, R. T. et al. Sexual dimorphism in bidirectional SR–mitochondria crosstalk in ventricular cardiomyocytes. *Basic Res. Cardiol.* **118**, 15 (2023).
309. Kamada, S., Takeiwa, T., Ikeda, K., Horie, K. & Inoue, S. Emerging roles of COX7RP and mitochondrial oxidative phosphorylation in breast cancer. *Front. Cell Dev. Biol.* **10**, 717881 (2022).
310. Fernández-Vizarra, E. et al. Two independent respiratory chains adapt OXPHOS performance to glycolytic switch. *Cell Metab.* **34**, 1792–1808.e1796 (2022).
311. Arieli, Y., Gursahani, H., Eaton, M. M., Hernandez, L. A. & Schaefer, S. Gender modulation of Ca^{2+} uptake in cardiac mitochondria. *J. Mol. Cell. Cardiol.* **37**, 507–513 (2004).
312. Chweih, H., Castilho, R. F. & Figueira, T. R. Tissue and sex specificities in Ca^{2+} handling by isolated mitochondria in conditions avoiding the permeability transition. *Exp. Physiol.* **100**, 1073–1092 (2015).
313. Tong, D. et al. Female sex is protective in a preclinical model of heart failure with preserved ejection fraction. *Circulation* **140**, 1769–1771 (2019).
314. Troy, A. M. et al. Impact of ovary-intact menopause in a mouse model of heart failure with preserved ejection fraction. *Am. J. Physiol. Heart Circ. Physiol.* **326**, H522–h537 (2024).
315. Abdellatif, M., Sedej, S. & Kroemer, G. NAD^+ Metabolism in cardiac health, aging, and disease. *Circulation* **144**, 1795–1817 (2021).
316. Lee, C. F. et al. Normalization of NAD^+ redox balance as a therapy for heart failure. *Circulation* **134**, 883–894 (2016).
317. Abdellatif, M. et al. Nicotinamide for the treatment of heart failure with preserved ejection fraction. *Sci. Transl. Med.* **13**, eabd7064 (2021).
318. Tong, D. et al. NAD^+ repletion reverses heart failure with preserved ejection fraction. *Circ. Res.* **128**, 1629–1641 (2021).
319. Koay, Y. C. et al. The efficacy of risk factor modification compared to NAD^+ repletion in diastolic heart failure. *JACC Basic Transl. Sci.* **9**, 733–750 (2024).
320. Liu, X. et al. Mitochondrial protein hyperacetylation underpins heart failure with preserved ejection fraction in mice. *J. Mol. Cell. Cardiol.* **165**, 76–85 (2022).
321. Wang, Y. C. et al. Indole-3-propionic acid protects against heart failure with preserved ejection fraction. *Circ. Res.* **134**, 371–389 (2024).
322. Loescher, C. M., Hobbach, A. J. & Linke, W. A. Titin (TTN): from molecule to modifications, mechanics, and medical significance. *Cardiovasc. Res.* **118**, 2903–2918 (2022).
323. Diguet, N. et al. Nicotinamide riboside preserves cardiac function in a mouse model of dilated cardiomyopathy. *Circulation* **137**, 2256–2273 (2018).
324. Walker, M. A. et al. Raising NAD^+ level stimulates short-chain dehydrogenase/reductase proteins to alleviate heart failure independent of mitochondrial protein deacetylation. *Circulation* **148**, 2038–2057 (2023).

325. Vignier, N. et al. Rescue of biosynthesis of nicotinamide adenine dinucleotide protects the heart in cardiomyopathy caused by lamin A/C gene mutation. *Hum. Mol. Genet.* **27**, 3870–3880 (2018).
326. Abdellatif, M. et al. Autophagy is required for the therapeutic effects of the NAD^+ precursor nicotinamide in obesity-related heart failure with preserved ejection fraction. *Eur. Heart J.* https://doi.org/10.1093/eurheartj/ehaf062 (2025).
327. Horton, J. L. et al. Mitochondrial protein hyperacetylation in the failing heart. *JCI Insight* **2**, e84897 (2016).
328. Wang, D. D. et al. Safety and tolerability of nicotinamide riboside in heart failure with reduced ejection fraction. *JACC Basic Transl. Sci.* **7**, 1183–1196 (2022).
329. Zhou, B. et al. Boosting NAD level suppresses inflammatory activation of PBMCs in heart failure. *J. Clin. Invest.* **130**, 6054–6063 (2020).
330. Psotka, M. A. et al. Cardiac calcitropes, myotropes, and mitotropes: JACC review topic of the week. *J. Am. Coll. Cardiol.* **73**, 2345–2353 (2019).
331. Haghighat, L., DeJong, C. & Teerlink, J. R. New and future heart failure drugs. *Nat. Cardiovasc. Res.* **3**, 1389–1407 (2024).
332. Lee, L., Horowitz, J. & Frenneaux, M. Metabolic manipulation in ischaemic heart disease, a novel approach to treatment. *Eur. Heart J.* **25**, 634–641 (2004).
333. Lee, L. et al. Metabolic modulation with perhexiline in chronic heart failure: a randomized, controlled trial of short-term use of a novel treatment. *Circulation* **112**, 3280–3288 (2005).
334. Abozguia, K. et al. Metabolic modulator perhexiline corrects energy deficiency and improves exercise capacity in symptomatic hypertrophic cardiomyopathy. *Circulation* **122**, 1562–1569 (2010).
335. George, C. H., Mitchell, A. N., Preece, R., Bannister, M. L. & Yousef, Z. Pleiotropic mechanisms of action of perhexiline in heart failure. *Expert Opin. Ther. Pat.* **26**, 1049–1059 (2016).
336. Maron, M. S. et al. Safety and efficacy of metabolic modulation with ninerafaxstat in patients with nonobstructive hypertrophic cardiomyopathy. *J. Am. Coll. Cardiol.* **83**, 2037–2048 (2024).
337. Lim, G. B. Benefits of ninerafaxstat in non-obstructive hypertrophic cardiomyopathy. *Nat. Rev. Cardiol.* **21**, 357 (2024).
338. Gibson, C. M. et al. EMBRACE STEMI study: a phase 2a trial to evaluate the safety, tolerability, and efficacy of intravenous MTP-131 on reperfusion injury in patients undergoing primary percutaneous coronary intervention. *Eur. Heart J.* **37**, 1296–1303 (2016).
339. Sabbah, H. N. et al. Chronic therapy with elamipretide (MTP-131), a novel mitochondria-targeting peptide, improves left ventricular and mitochondrial function in dogs with advanced heart failure. *Circ. Heart Fail.* **9**, e002206 (2016).
340. Daubert, M. A. et al. Novel mitochondria-targeting peptide in heart failure treatment: a randomized, placebo-controlled trial of elamipretide. *Circ. Heart Fail.* **10**, e004389 (2017).
341. Butler, J. et al. Effects of elamipretide on left ventricular function in patients with heart failure with reduced ejection fraction: the PROGRESS-HF phase 2 trial. *J. Card. Fail.* **26**, 429–437 (2020).
342. Mortensen, S. A. et al. The effect of coenzyme Q10 on morbidity and mortality in chronic heart failure: results from Q-SYMBIO: a randomized double-blind trial. *JACC Heart Fail.* **2**, 641–649 (2014).
343. McDonagh, T. A. et al. 2021 ESC Guidelines for the diagnosis and treatment of acute and chronic heart failure. *Eur. Heart J.* **42**, 3599–3726 (2021).
344. Xu, J. et al. Efficacy and safety of coenzyme Q10 in heart failure: a meta-analysis of randomized controlled trials. *BMC Cardiovasc. Disord.* **24**, 592 (2024).
345. Spertus, J. A. et al. Mavacamten for treatment of symptomatic obstructive hypertrophic cardiomyopathy (EXPLORER-HCM): health status analysis of a randomised, double-blind, placebo-controlled, phase 3 trial. *Lancet* **397**, 2467–2475 (2021).
346. Bertero, E. et al. Real-world candidacy to mavacamten in a contemporary hypertrophic obstructive cardiomyopathy population. *Eur. J. Heart Fail.* **26**, 59–64 (2024).
347. Teerlink, J. R. et al. Effect of ejection fraction on clinical outcomes in patients treated with omecamtiv mecarbil in GALACTIC-HF. *J. Am. Coll. Cardiol.* **78**, 97–108 (2021).
348. Voors, A. A. et al. Effects of danicamtiv, a novel cardiac myosin activator, in heart failure with reduced ejection fraction: experimental data and clinical results from a phase 2a trial. *Eur. J. Heart Fail.* **22**, 1649–1658 (2020).
349. US National Library of Medicine. *ClinicalTrials.gov* https://www.clinicaltrials.gov/ct2/show/NCT06736574 (2025).
350. Chen, S. et al. Empagliflozin prevents heart failure through inhibition of the NHE1–NO pathway, independent of SGLT2. *Basic Res. Cardiol.* **119**, 751–772 (2024).
351. Chen, S. et al. Sodium glucose cotransporter-2 inhibitor empagliflozin reduces infarct size independently of sodium glucose cotransporter-2. *Circulation* **147**, 276–279 (2023).
352. Baartscheer, A. et al. Empagliflozin decreases myocardial cytoplasmic Na^+ through inhibition of the cardiac Na^+/H^+ exchanger in rats and rabbits. *Diabetologia* **60**, 568–573 (2017).
353. Uthman, L. et al. Class effects of SGLT2 inhibitors in mouse cardiomyocytes and hearts: inhibition of Na^+/H^+ exchanger, lowering of cytosolic Na^+ and vasodilation. *Diabetologia* **61**, 722–726 (2018).
354. Hegyi, B. et al. Empagliflozin reverses late Na^+ current enhancement and cardiomyocyte proarrhythmia in a translational murine model of heart failure with preserved ejection fraction. *Circulation* **145**, 1029–1031 (2022).
355. Mustroph, J. et al. Empagliflozin reduces Ca/calmodulin-dependent kinase II activity in isolated ventricular cardiomyocytes. *ESC Heart Fail.* **5**, 642–648 (2018).
356. Mustroph, J. et al. Empagliflozin inhibits cardiac late sodium current by Ca/calmodulin-dependent kinase II. *Circulation* **146**, 1259–1261 (2022).
357. McDonagh, T. A. et al. 2023 focused update of the 2021 ESC guidelines for the diagnosis and treatment of acute and chronic heart failure. *Eur. Heart J.* **44**, 3627–3639 (2023).
358. KDIGO 2024 clinical practice guideline for the evaluation and management of chronic kidney disease. *Kidney Int.* https://doi.org/10.1016/j.kint.2023.10.018 (2024).
359. Frías, J. P. et al. Tirzepatide versus semaglutide once weekly in patients with type 2 diabetes. *N. Engl. J. Med.* **385**, 503–515 (2021).
360. Borlaug, B. A. et al. Effects of tirzepatide on circulatory overload and end-organ damage in heart failure with preserved ejection fraction and obesity: a secondary analysis of the SUMMIT trial. *Nat. Med.* **31**, 544–551 (2025).
361. Kramer, C. M. et al. Tirzepatide reduces LV mass and paracardiac adipose tissue in obesity-related heart failure: SUMMIT CMR substudy. *J. Am. Coll. Cardiol.* **85**, 699–706 (2025).
362. Desai, M. Y. et al. Myosin inhibition in patients with obstructive hypertrophic cardiomyopathy referred for septal reduction therapy. *J. Am. Coll. Cardiol.* **80**, 95–108 (2022).
363. Tian, Z. et al. Effect of mavacamten on Chinese patients with symptomatic obstructive hypertrophic cardiomyopathy: the EXPLORER-CN randomized clinical trial. *JAMA Cardiol.* **8**, 957–965 (2023).

Acknowledgements

This Review is based on work supported by the COST Action EU-METAHEART CA22169 supported by COST (European Cooperation in Science and Technology). D.A. is supported by a Wellcome Trust Career Re-Entry Fellowship (221604/Z/20/Z), Barts Charity Grant (G-002145) and Fondation Pour la Recherche en Physiologie. S.S. and M.A. are supported by the Austrian Science Fund (FWF) for excellence cluster 10.55776/COE14, the Medical University of Graz (Excellence Cluster MetAGE and Flagship Project VASC-HEALTH) and BioTechMed-Graz (Flagship Project INTERACD* to S.S. and Young Researcher Group to M.A.). M.A. acknowledges additional funding received from the FWF (DOI: 10.55776/P34926) as well as (DOI: 10.55776/I6931) under the umbrella of the Partnership Fostering a European Research Area for Health (ERA4Health) (GA no. 101095426 of the EU Horizon Europe Research and Innovation Programme). J.F. is supported by the Fondation de France (no. 00056858/00121055) and Agence National de La Recherche, ANR CALMOS (ANR-18-CE17-0003), ANR MiMeTiC (ANR-20-CE18-0035) and ANR MASTERMIND (ANR-22-CE14-0025). M.P. is supported by grants from Fondation de France (no. 00107048) and from the Agence Nationale de la Recherche (ANR-20-CE14-0013-01). K.S.-B. is supported by the German Research Foundation (Deutsche Forschungsgemeinschaft (DFG)) with the Collaborative Research Center (CRC) 1213 (SFB/CRC 1213/B07), the RTG 2824/P04 and the project number 471241922. J.v.d.V. acknowledges support from NWO-ZonMW (91818602 VICI grant), ZonMW and Heart Foundation for the translational research programme, project 95105003; the Dutch Cardiovascular Alliance (DCVA) grant Double Dose 2021; and the Leducq Foundation grant number 20CVD01. R.A.d.B. is supported by the Netherlands Heart Foundation (NHS grants Double Dose 2020B005; 01-003-2022-0358), by an NHS grant co-funded by ERA4Health (GA grant 101095426 of the EU Horizon Europe Research and Innovation Programme) and by the European Research Council (ERC CoG 818715, SECRETE HF). J.D. is funded by the DFG (SFB1525; project no. 453989101) and the Interdisziplinäres Zentrum für Klinische Forschung (IZKF; E-457). V.S. received postdoctoral funding from the Japanese Society for the Promotion of Science (JSPS; S23089) and the DFG (project nos. 530849567 and 554784412). C.M. is funded by the DFG (SFB-1525/project no. 453989101 and Ma: 2528/8-1) and the German Center for Cardiovascular Research (DZHK; EX-22 and FKZ 81×2800227).

Author contributions

D.A., S.S., J.F., M.P., M.A., K.S.-B., R.V.-C., J.v.d.V., E.B., V.S. and C.M. contributed substantially to all aspects of the article. R.A.d.B and J.D. contributed to writing the manuscript.

Competing interests

D.A. reports a research agreement with AstraZeneca. S.S. and M.A. hold a patent related to the cardiometabolic effects of nicotinamide and spermidine. M.P. reports a collaborative study with Boehringer Ingelheim. K.S.-B. has received grants from BionTech and Novartis and has received speaker's honoraria from Novartis. R.A.d.B. has had speaker engagements with and/or received fees from and/or served on an advisory board for Abbott, AstraZeneca, Bristol Myers Squibb, NovoNordisk, Roche and Zoll; he has received travel support from Abbott and NovoNordisk, and his institution has received research grants and/or fees from Abbott, Alnylam, AstraZeneca, Bristol Myers Squibb, NovoNordisk and Roche; V.S. has received research funding from Bristol Myers Squibb. C.M. is an advisory board member or speaker for Amgen, AstraZeneca, Bayer, Berlin Chemie, Boehringer Ingelheim, Bristol Myers Squibb, Cytokinetics, Edwards, Lilly, Novartis, NovoNordisk and Servier. The other authors declare no competing interests.

Additional information

Peer review information *Nature Reviews Cardiology* thanks Genevieve Sparagna and the other, anonymous, reviewer(s) for their contribution to the peer review of this work.

Publisher's note Springer Nature remains neutral with regard to jurisdictional claims in published maps and institutional affiliations.

Springer Nature or its licensor (e.g. a society or other partner) holds exclusive rights to this article under a publishing agreement with the author(s) or other rightsholder(s); author self-archiving of the accepted manuscript version of this article is solely governed by the terms of such publishing agreement and applicable law.

© Springer Nature Limited 2025

[1]William Harvey Research Institute, Bart's Faculty of Medicine and Dentistry, Queen Mary University of London, London, UK. [2]Department of Cardiology, Medical University of Graz, Graz, Austria. [3]BioTechMed–Graz, Graz, Austria. [4]Faculty of Medicine, University of Maribor, Maribor, Slovenia. [5]PhyMedExp, University of Montpellier, INSERM U1046, CNRS UMR 9214, Montpellier, France. [6]University Claude Bernard Lyon 1, CarMeN Laboratory–IRIS Team, INSERM INRAE, Bron, France. [7]Centre de Recherche des Cordeliers, Equipe Labellisée par la Ligue Contre le Cancer, Université de Paris, Sorbonne Université, INSERM U1138 Institut Universitaire de France, Paris, France. [8]Institute of Pharmacology and Toxicology, Julius Maximilians University, Würzburg, Germany. [9]Medical Clinic I, Cardiology and Angiology, Justus Liebig University, Giessen, Germany. [10]Faculté de Pharmacie, Université Paris-Saclay, Bât Henri Moissan UMR-S 1180, Orsay, France. [11]Department of Physiology, Amsterdam Cardiovascular Sciences, Amsterdam UMC, Vrije Universiteit, Amsterdam, The Netherlands. [12]Erasmus Medical Center, CardioVascular Research Institute, Thorax Center, Department of Cardiology, Rotterdam, The Netherlands. [13]Cardiovascular Unit, Department of Internal Medicine, University of Genova, Genova, Italy. [14]Comprehensive Heart Failure Center Würzburg, Würzburg, Germany. [15]Medical Clinic 1, University Clinic Würzburg, Würzburg, Germany.